AD_____

Award Number: W81XWH-06-1-0572

TITLE: Novel Breast Cancer Therapeutics Based on Bacterial Cupredoxin

PRINCIPAL INVESTIGATOR: Pernilla Wittung-Stafshede, Ph.D.

CONTRACTING ORGANIZATION: Rice University
Houston, TX 77521

REPORT DATE: September 2007

TYPE OF REPORT: Annual

PREPARED FOR: U.S. Army Medical Research and Materiel Command
Fort Detrick, Maryland 21702-5012

DISTRIBUTION STATEMENT: Approved for Public Release;
Distribution Unlimited

REPORT DOCUMENTATION PAGE

Form Approved
OMB No. 0704-0188

1. REPORT DATE *(DD-MM-YYYY)*	**2. REPORT TYPE**	**3. DATES COVERED** *(From - To)*
01-09-2007	Annual	15 AUG 2006 - 14 AUG 2007

4. TITLE AND SUBTITLE
Novel Breast Cancer Therapeutics Based on Bacterial Cupredoxin

5a. CONTRACT NUMBER

5b. GRANT NUMBER
W81XWH-06-1-0572

5c. PROGRAM ELEMENT NUMBER

6. AUTHOR(S)
Pernilla Wittung-Stafshede, Ph.D.

E-Mail: pernilla@rice.edu

5d. PROJECT NUMBER

5e. TASK NUMBER

5f. WORK UNIT NUMBER

7. PERFORMING ORGANIZATION NAME(S) AND ADDRESS(ES)

Rice University
Houston, TX 77521

8. PERFORMING ORGANIZATION REPORT NUMBER

9. SPONSORING / MONITORING AGENCY NAME(S) AND ADDRESS(ES)
U.S. Army Medical Research and Materiel Command
Fort Detrick, Maryland 21702-5012

10. SPONSOR/MONITOR'S ACRONYM(S)

11. SPONSOR/MONITOR'S REPORT NUMBER(S)

12. DISTRIBUTION / AVAILABILITY STATEMENT
Approved for Public Release; Distribution Unlimited

13. SUPPLEMENTARY NOTES

14. ABSTRACT The tumor suppressor p53 is a major player in cell growth, genomic stability and cell death. Recent *in vivo* work suggested that bacterial *Pseudomonas aeruginosa* azurin can enter cancer cells and interact with p53 promoting cell death. Despite being a novel concept to target cancer, there are no thermodynamic details known for the proposed azurin-p53 complex. This project aims to fill this gap by employing biophysical methods in conjunction with purified proteins *in vitro* to address four aims. We will reveal (1.) which p53 domain interacts with azurin and probe affinity and stoichiometry, (2.) the molecular mechanism by which azurin increases cellular levels of p53, (3.) the region on azurin that interacts with p53 and (4.) use the acquired information to propose smaller molecules that retain properties of azurin. During the year, several discoveries have been made: most importantly, azurin is found to bind to the unstructured N-terminal domain of p53 and a small 13-residue peptide is able to reproduce part of the azurin interaction. Better biophysical understanding of azurin's interaction with p53 *in vitro* may be the gateway to innovative treatments of cancer.

15. SUBJECT TERMS
p53, azurin, spectroscopy, calorimetry, peptide, copper

16. SECURITY CLASSIFICATION OF:			**17. LIMITATION OF ABSTRACT**	**18. NUMBER OF PAGES**	**19a. NAME OF RESPONSIBLE PERSON**
a. REPORT	**b. ABSTRACT**	**c. THIS PAGE**			USAMRMC
U	U	U	UU	35	**19b. TELEPHONE NUMBER** *(include area code)*

Table of Contents

Introduction

The p53 tumor suppressor protein is involved in multiple central cellular processes, including transcription, DNA repair, genomic stability, cell cycle control and apoptosis; it is functionally inactivated by structural mutations, interaction with viral products and endogenous cellular mechanisms in many human cancers (1). *P. aeruginosa* azurin, a copper-containing redox protein (2), was recently discovered to enter mammalian cells and either induce apoptosis (wild-type) or inhibit cell-cycle progression (Met44LysMet64Glu azurin variant). Azurin specifically entered J774 cells, derived from murine reticulum cell sarcoma (3), and cancer cell lines such as melanoma UISO-Mel-2 cells and MCF-7 breast-cancer cells and caused cell death (4-7). In both instances, azurin formed a complex with the tumor suppressor protein p53, thereby somehow raising its intracellular level. High levels of p53 then triggered apoptosis in the cells through enhanced Bax formation and the release of mitochondrial cytochrome c to the cytosol. In addition, azurin was able to inhibit tumor growth in xeno-transplanted nude mice without toxicity symptoms. The support for the presence of a direct azurin-p53 complex was based on glycerol-gradient ultracentrifugation and pull-down experiments using GST-fusion constructs (7-9).

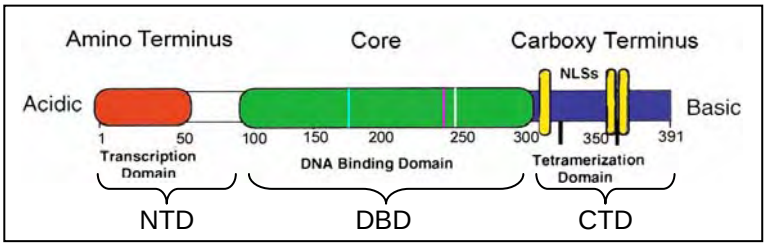

Figure 1. The diagram shows arrangements of domains in p53. Red, transcription domain which is part of NTD; green, DNA-binding domain DBD; blue, tetramerization domain which is part of CTD.

p53 is a 393-residue protein (1) that can be divided into three structural domains (Figure 1): (i) A transcription activation segment and a proline-rich segment form the N-terminal domain (NTD; residues 1-93). (ii) A DNA-binding domain which adopts a β-sheet structure and coordinates a zinc ion (DBD; residues 102-292). (iii) A helical tetramerization domain which together with a sequence-unspecific DNA-binding domain form the C-terminal domain (CTD; residues 293-393). Biophysical experiments have shown that NTD and CTD are mostly unstructured, whereas DBD is well folded, in solution (10-12). Under "latent" conditions, CTD interacts with DBD, preventing it from recognizing target DNA. In addition, p53 can bind proteins through its NTD (*e.g.*, mouse double minute 2 homolog (MDM2) and jun-kinase (JNK)) which mediate the targeting of p53 to the proteasome for

rapid degradation (*1, 13*). Thus, p53 is not only hindered from binding to DNA but it is also very unstable and rapidly disappears from the cell at non-stress conditions. Various stimuli are capable of releasing these interactions which result in a conformational change in p53 that exposes the DBD and allows for p53-mediated transcriptional activation (*1, 14, 15*).

Pseudomonas aeruginosa azurin is a 128-residue, blue-copper protein (also called cupredoxin) that is believed to facilitate electron transfer in denitrification/respiration chains (2). It was recently proposed that the physiological function of azurin in *P. aeruginosa* involves electron transfer directly related to the cellular response to oxidative stress (*16*). Azurin (Figure 2) has one α-helix and eight β-strands that fold into a rigid β-barrel structure arranged in a double-wound Greek-key topology (*2, 17*).

Figure 2. Ribbon structure of azurin (1AZU), with copper shown in blue space-filling and the five copper-ligands (Gly45, His46, Cys112, His117 and Met121) in stick representation.

In vivo, azurin coordinates a redox-active copper (Cu^{II}/Cu^{I}) *via* two histidine imidazoles, one cysteine thiolate, and two weaker axial ligands, sulfur of methionine and carbonyl of glycine in a trigonal bipyramidal geometry (Figure 2). The highly covalent nature of the copper-cysteine bond gives azurin an intense absorption at 630 nm (2). The copper in azurin can be eliminated, creating apo-azurin, or exchanged for other metals *in vitro* without change of the overall structure (*17, 18*). We have studied azurin extensively over the years as a model system to address the role of metals in protein folding (*19-27*).

Here, we employ a battery of biophysical tools and purified proteins to investigate molecular, structural and thermodynamic details of the azurin-p53 complex *in vitro*. Below follows a description of the progress we have made on the four different tasks outlined in the original Statement of Work.

Task 1. ***Determine which p53 domain interacts with azurin and probe the affinity and stoichiometry of the complex in vitro***

Experiments have shown that the NTD domain is natively unfolded whereas full-length p53 (which is tetrameric at μM concentrations) exhibits high stability *in vitro* (*10,*

11). Also, p53's C-terminal domain appears to have unstructured regions (12). Earlier experiments, using fusion proteins and glycerol gradients, have suggested that *P. aeruginosa* azurin binds to the central or N-terminal portion of p53 (7-9). Therefore, we first prepared the NTD domain (i.e., residues 1-93 of p53). The protein was purified by standard methods as described in (11). Next, NTD was tested for azurin binding via isothermal titration calorimetry (ITC) to directly obtain stoichiometry and affinity of a potential azurin-NTD complex. From the data (Figure 3), it is clear that NTD does interact with azurin (pH 7.5, 25 ºC). The thermogram reveals a dissociation constant (K_D) of about 300 nM and a stoichiometry of 2 azurin molecules per NTD. From additional experiments, we found that the affinity remained the same also at 37 ºC, but decreased about 10-fold if the salt was removed from the buffer. The latter result suggests that hydrophobic interactions are important for azurin binding to p53/NTD.

In earlier work (*28*), we used ITC to probe the complex between full-length p53 and azurin. We then revealed that the complex involved four azurin molecules per p53 monomer; the dissociation constant (K_D) for each site was 33±12 nM (pH 7.5, 25ºC). Thus, the new data suggest that NTD is the site in p53 for azurin binding; nonetheless, the other p53 domains may also play a role (perhaps via long-range interactions/conformational changes) as the stoichiometry and affinity of azurin binding differs between the full-length and NTD p53 constructs.

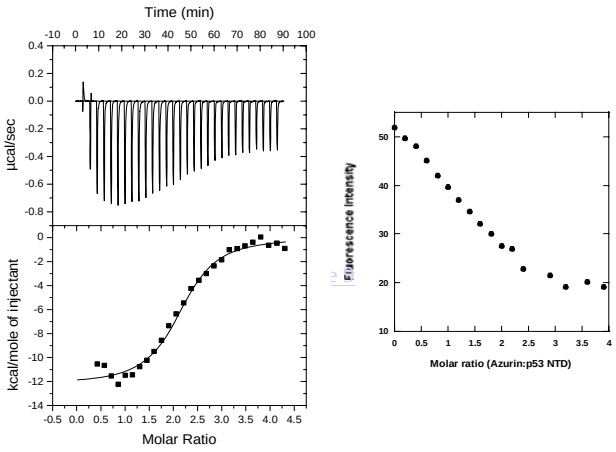

Figure 3. Left. ITC data showing the raw heat injections on top and, below, the thermogram with the integrated enthalpy as a function of azurin:NTD ratio. The solid curve is the best fit to the data. 5 µM NTD (in cell) was titrated with azurin (in syringe) in a buffer of 20 mM phosphate, 300 mM NaCl, pH 7.5, 20 °C. **Right.** Fluorescence at 350 nm of NTD (excitation at 295 nm; i.e. Trp) as a function of added Cu-azurin. The solvent conditions are the same as in the ITC experiments. Background emission from Cu-azurin was subtracted.

Each p53 monomer contains four tryptophan residues: three in the NTD (Trp23, Trp53, Trp91) and one in the DBD (Trp146). The tryptophan in the DBD is highly quenched due to nearby charges; also the other tryptophans show weak emission, which has been explained by solvent exposure (*29*). Azurin has one tryptophan (Trp48) whose

emission is highly quenched by the copper (*30*). Upon addition of the copper-form of azurin, we find NTD's tryptophan emission to decrease by ~ 70 % until a stoichiometry of 2:1 is reached (Figure 3). This result supports that when azurin molecules bind to NTD, the copper ions are positioned near the tryptophans so that metal-induced quenching can take place. We also tested if NTD's far-UV CD signal was affected by azurin binding. NTD is unstructured in the absence of azurin, however upon addition of 2-fold excess azurin, the negative CD signal around 210-220 nm from NTD grows larger indicating gain of structure (not shown). Further studies are needed to elucidate the nature of the increase, *i.e.* if it is helical or β-sheet type of structure that forms. Preliminary infra-red (IR) spectroscopic studies of the NTD-azurin interactions suggest that β-sheet structure is formed. To reveal if some azurin molecules bind to the other p53 domains, future studies will include preparation and studies of the DBD and CTD domains of p53.

Task 2. ***Elucidate the molecular mechanism by which azurin may increase cellular levels of p53***

We propose that the increased cellular levels of p53 observed in the presence of azurin may be due to (*i*) increased intrinsic stability of p53, (*ii*) steric shielding of p53 from degradation enzymes or (*iii*) enhanced DNA-binding capacity. To reveal the molecular mechanism behind azurin's ability to promote p53-mediated cell death in cancer cells, we have investigated all three possibilities *in vitro* using full-length p53 and azurin.

Azurin's effect on p53's intrinsic thermodynamic stability was probed by equilibrium-unfolding experiments using GuHCl and temperature perturbations. Since there has been some conflicting reports on wild-type p53 stability (*11, 12*), we first clarified this issue at our conditions. The observation on p53 in isolation was compared to unfolding data when in complex with azurin. p53 was found to unfold before azurin (*i.e.*, at lower denaturant concentration and at lower temperature). This is reasonable since the copper-form of azurin has an usually high stability (52 kJ/mol, pH 7): its GuHCl-unfolding midpoint is ~4.5 M and it is thermally stable up to at least 75°C (*21, 31*). Unfolding of p53 was monitored by far-UV CD (*32*).

Our experiments showed that the thermal stability of full-length p53 as monitored by far-UV CD is not increased by azurin-complex formation (Figure 4). In agreement with published data on full-length p53 (*29*), the unfolding midpoint for p53 appeared at 65ºC and the unfolded state retains some secondary structure. In the presence of azurin, the midpoint shifts downwards by 5ºC; moreover, p53 unfolding becomes more complete (*i.e.* unfolded state appears more random-coil like). This implies (*i*) that azurin remains bound throughout p53's thermal transition, (*ii*) that the presence of bound azurin restricts long-range interactions that somewhat stabilize the native structure of p53 and, finally, (*iii*) that bound azurin limits retention of secondary-structure elements in the unfolded state. In analogy, the GuHCl-induced unfolding experiments at room-temperature revealed that also p53's thermodynamic stability towards chemical perturbation is not enhanced by the interaction with azurin. Based on these findings, the increased cellular levels of p53 in the presence of azurin are *not* due to increased wild-type p53 stability.

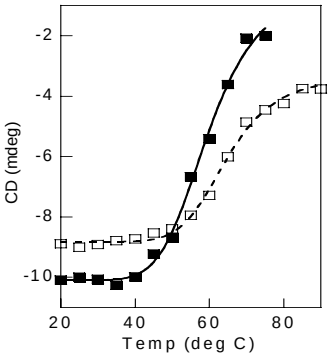

Figure 4. Thermal transitions monitored by CD at 218 nm for p53 alone (open symbols) and p53 in complex with azurin (filled symbols; azurin signals subtracted). Note that azurin (copper-form) does not unfold until above 75ºC.

Several inactivating enzymes bind to p53's NTD, thus masking the transcription activation segment. For example, the MDM2 protein is overactive in many tumors; its binding to the NTD results in p53 inactivation and degradation (13). If azurin binds to NTD, as suggested by the results in Task 1, its binding-site may overlap with those of inactivation and degradation proteins and, therefore, bound azurin molecules may sterically shield p53 from interacting with such proteins. Depending on the relative p53 affinities, azurin may even displace degradation and inactivation proteins from p53. To address this hypothesis *in vitro*, we performed proteolysis experiments of full-length p53 in the presence and absence of azurin. Chymotrypsin, that hydrolyses peptide bonds involving tyrosines, phenylalanines and tryptophans, as well as trypsin, that is specific to lysines and arginines, was employed. p53 has four tryptophans, nine tyrosines, ten phenylalanines and forty-six residues that are either lysine or arginine. Extent of cleavage was monitored as a function of time and detected by standard gel-electrophoresis methods. Despite a large

number of experiments in which we varied enzyme concentration, solvent conditions and temperature, we never detected any differences in the proteolytic pattern of p53 as a function of the presence/absence of azurin. Thus, at least with respect to chymotrypsin and trypsin, azurin binding does not protect p53 towards degradation.

We plan to test azurin binding to full-length p53 in the presence of the p53-binding domain of MDM2 by gel-filtration and ITC experiments. This will reveal if the binding sites for azurin and MDM2 overlap and, if so, whether azurin can competitively displace MDM2. We have so far successfully purified the MDM2 protein in the lab.

To investigate the effect of azurin on p53's DNA-binding ability, we used a 20 base-pair DNA duplex (5'-AGGCATGTCTAGGCATGTCT-3' and 3'-TCCGTACAGATCCGTACAGA-5' oligonucleotides annealed) that contains the consensus sequence for p53 binding. We employed ITC to first reveal the affinity between p53 and the DNA target at our conditions. Next we tested p53's ability to bind DNA in the presence of azurin (Figure 5). Stronger DNA binding in the presence of azurin would provide a mechanistic explanation for how azurin mediates p53-induced apoptosis *in vivo*. However, we did not observe tighter binding in the presence of azurin; in fact, the presence of azurin did not affect the DNA binding of p53 to any degree (the dissociation constant for the p53-DNA complex was 50±20 nM both with and without azurin; pH 7.5, 20 ºC). This result provides further support that azurin binds to NTD, which is a domain that is not involved in DNA binding.

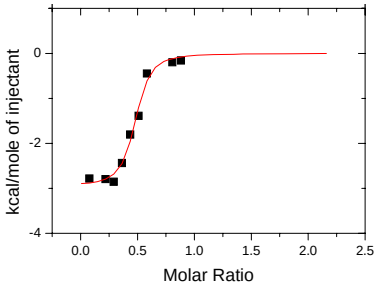

Figure 5. ITC data showing the integrated enthalpy as a function of DNA:p53 ratio. The solid curve is the best fit to the data. 5 μM p53 with 25 μM azurin (in cell) was titrated with pre-formed DNA duplex (in syringe) in a buffer of 350 mM phosphate, 150 mM NaCl, pH 7.5, 20 °C. The data analysis give a dissociation constant of about 50 nM and a stoichiometry of about 1 DNA duplex per two p53. The same parameters were found in the absence of azurin.

Task 3. ***Define the surface on azurin that interacts with p53 and reveal the role of azurin's metal cofactor in p53 binding***

We have made preliminary comparisons of the interactions between p53 and apo-, zinc- and copper-forms of azurin, respectively, by ITC. It appears that the presence of a metal (Cu or Zn) is favorable for high affinity but that the apo-form of azurin can also bind

to p53. It has earlier been shown that two residues in azurin (Met44 and Met64) are important for complex formation with p53. In contrast to wild-type azurin, the Met44LysMet64Glu double-mutant of azurin did not bind p53 (4-7). We plan to prepare a set of azurin surface mutants, focusing on residues in azurin's hydrophobic patch which include Met44 and Met64. This is the surface area of azurin known to be involved in interactions with other redox proteins *in vitro* (*33*). After preparation, the variants will be tested for p53 binding by ITC and gel-filtration experiments. We have made complementary progress on identifying what parts of azurin interacts with p53 through the peptide work described under task 4 below.

To explore the biological consequences of a possible need for the copper-form of azurin for tight binding to p53, we investigated the effects of copper on the structure and stability of two human proteins that participate in copper metabolism pathways. These proteins could be involved in interactions with azurin, that may result in azurin de-metallation or hinder azurin to reach p53, if azurin (or variants) are to be used as cancer drugs in the future. One of the proteins (*i.e.,* ceruloplasmin) has the same fold as azurin but contains 6 such domains and functions in the plasma, whereas the other protein (*i.e.*, copper-chaperone Atox1) has a different fold and is responsible for copper transport in the cytoplasm. Before assessing how these proteins may interact with azurin, it is required to elucidate their individual properties. The results of such thermodynamic characterizations are described in two manuscripts in press in *Biochemisty* and *Biochem Biophys Acta* (*34*, *35*). We note that in addition to their relevance to azurin and the purpose of targeting p53, these proteins may be over-expressed in many cancers as it has been proposed that copper accumulates in tumors.

Task 4. ***Use the acquired information on the complex to design small peptide variants that retain the ability to bind and affect p53 like full-length azurin***

The acquired information from the work in Tasks 1-3 will ultimately be used to design peptide variants that mimic azurin's interaction with p53. In contrast to full-length proteins, small peptides are not expected to trigger immunological responses when introduced into a host organism. Moreover, there are strategies to deliver peptides into cells

(for example by linkage to a harmless protein that can breach cell membranes) and ways to eliminate peptide vulnerability to degradation (*36-38*).

To date, we have tested a small 13-residue peptide corresponding to azurin's C-terminal sequence, *i.e.*, residues 111-124 with the sequence F**C**TFPG**H**SAL**M**KG (*19, 39*). This peptide contains three key residues involved in azurin's copper site, Cys112, His117 and Met 121 (bold in above sequence). The peptide was tested for p53 and NTD binding with and without the presence of copper (Figure 6). We found that the Cu-loaded peptide binds to p53 in a 1:1 stoichiometry and a K_D of about 100 nM was estimated (pH 8, 20 °C). This is only 25-fold weaker binding than full-length azurin binding to p53. The Cu-peptide complex could also bind to NTD in a 1:1 stoichiometry although the affinity was now reduced to correspond to a K_D of about 2.6 μM. Nonetheless, this is only 10-fold weaker than full-length azurin's affinity for NTD. The peptide binding was reduced if Cu was removed. In the absence of copper, the K_D of the peptide for p53 was 600 nM and no peptide interaction with NTD could be detected (Figure 6). The control experiments testing if copper alone could bind to p53 was negative, indicating no such interaction. Key thermodynamic parameters are listed in Table 1.

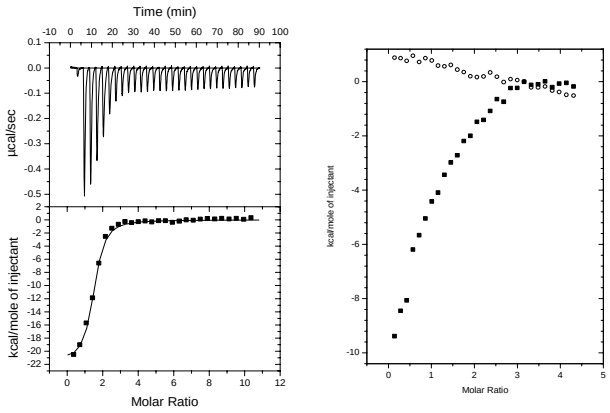

Figure 6. Left. ITC data showing the raw heat injections on top and, below, the thermogram with the integrated enthalpy as a function of peptide:p53 ratio. The solid curve is the best fit to the data. 2 μM p53 (in cell) was titrated with Cu-peptide (in syringe) in a buffer of 100 mM phosphate, pH 8, 20 °C. **Right.** Comparison of thermograms for peptide additions to NTD with (filled symbols) and without (open symbols) pre incubation with Cu.

These results have several implications. First, they suggest that it is the area around the metal site in azurin that interacts with p53. Second, they suggest that metal-induced secondary structure in the peptide is important for tight binding, in agreement with specific binding sites on p53. Third, since peptide binding occurs also to NTD, it strengthens the conclusion that full-length azurin also binds to NTD. Finally, these observations indicate that peptide mimics can reproduce (at least part of) the azurin-p53 interaction. Future cell culture studies will test the ability of this peptide to penetrate cancer cells, interact with

p53, and thereby trigger apoptosis. For this, we will turn to a collaborator for help. If peptide-based constructs can be found that bind to p53 like full-length azurin and triggers apoptosis *in vivo*, they will be novel leads for the development of new cancer drugs.

Table 1. Summary of auzin/peptide interactions with p53/NTD (pH 7.5-8.0, 20 °C).

Azurin variant	Variant of p53	K_D	Stoichiometry
Cu-azurin	p53	40 nM	4:1
Apo-peptide	p53	600 nM	1:1
Cu-peptide	p53	100 nM	1:1
Cu-azurin	NTD	300 nM	2:1
Apo-peptide	NTD	*No binding*	-
Cu-peptide	NTD	2.6 μM	1:1

Key research accomplishments

- Copper-form of azurin binds to NTD domain of p53 with nM affinity
- Stoichiometry of azurin-NTD complex (i.e., 2:1) differs from that of azurin-p53 (i.e., 4:1) indicating that other p53 domains play some role in interaction
- Azurin binding does not increase p53 stability, protect p53 against proteases or affect p53's DNA binding
- Peptide corresponding to copper-binding segment of azurin binds to p53 similarly to full-length azurin; Cu is required for this
- Properties of two human copper-metabolism proteins have been identified; these proteins are important as they may cross-react with azurin-based drugs

Reportable outcomes

- Two manuscripts accepted (see Appendix)
- One paper on peptide/NTD binding data in preparation
- Training of postdocs; one got a research position at National lab due to this work
- Increased interest to join research group from incoming students
- Initiation of new collaborations; widening of research scope

Conclusion/"So what?"

Reports of regression of cancer in humans infected with microbial pathogens date back more than 100 years (3). However, live bacteria produce significant toxicity, limiting their use. The unprecedented observation that the small bacterial protein *P. aeruginosa*

azurin forms a complex with the well-known tumor suppressor protein p53 and triggers cell death provides *a new avenue for cancer research*. Our biophysical project provides key physical, chemical and structural understanding of azurin's interaction with p53 *in vitro*. We propose that the results of our studies may be used to develop small peptide constructs that bind and stabilize p53 like full-length azurin. If these molecules turn out to work *in vivo*, it may be the gateway to an innovative class of new cancer therapeutics.

References

(1) Harris, C. C. (1996) Structure and function of the p53 tumor suppressor gene: clues for rational cancer therapeutic strategies. *J Natl Cancer Inst 88*, 1442-1455.

(2) Adman, E. T. (1991) Copper protein structures. *Adv Protein Chem 42*, 145-197.

(3) Yamada, T., Goto, M., Punj, V., Zaborina, O., Chen, M. L., Kimbara, K., Majumdar, D., Cunningham, E., Das Gupta, T. K., and Chakrabarty, A. M. (2002) Bacterial redox protein azurin, tumor suppressor protein p53, and regression of cancer. *Proc Natl Acad Sci U S A 99*, 14098-14103.

(4) Goto, M., Yamada, T., Kimbara, K., Horner, J., Newcomb, M., Gupta, T. K., and Chakrabarty, A. M. (2003) Induction of apoptosis in macrophages by Pseudomonas aeruginosa azurin: tumour-suppressor protein p53 and reactive oxygen species, but not redox activity, as critical elements in cytotoxicity. *Mol Microbiol 47*, 549-559.

(5) Punj, V., Das Gupta, T. K., and Chakrabarty, A. M. (2003) Bacterial cupredoxin azurin and its interactions with the tumor suppressor protein p53. *Biochem Biophys Res Commun 312*, 109-114.

(6) Yamada, T., Goto, M., Punj, V., Zaborina, O., Kimbara, K., Das Gupta, T. K., and Chakrabarty, A. M. (2002) The bacterial redox protein azurin induces apoptosis in J774 macrophages through complex formation and stabilization of the tumor suppressor protein p53. *Infect Immun 70*, 7054-7062.

(7) Yamada, T., Hiraoka, Y., Ikehata, M., Kimbara, K., Avner, B. S., Das Gupta, T. K., and Chakrabarty, A. M. (2004) Apoptosis or growth arrest: Modulation of tumor suppressor p53's specificity by bacterial redox protein azurin. *Proc Natl Acad Sci U S A 101*, 4770-4775.

(8) Punj, V., Bhattacharyya, S., Saint-Dic, D., Vasu, C., Cunningham, E. A., Graves, J., Yamada, T., Constantinou, A. I., Christov, K., White, B., Li, G., Majumdar, D., Chakrabarty, A. M., and Das Gupta, T. K. (2004) Bacterial cupredoxin azurin as an inducer of apoptosis and regression in human breast cancer. *Oncogene 23*, 2367-2378.

(9) Yamada, T., Hiraoka, Y., Das Gupta, T. K., and Chakrabarty, A. M. (2004) Regulation of mammalian cell growth and death by bacterial redox proteins: relevance to ecology and cancer therapy. *Cell Cycle 3*, 752-755.

(10) Dawson, R., Muller, L., Dehner, A., Klein, C., Kessler, H., and Buchner, J. (2003) The N-terminal domain of p53 is natively unfolded. *J Mol Biol 332*, 1131-1141.

(11) Nichols, N. M., and Matthews, K. S. (2001) Protein-DNA binding correlates with structural thermostability for the full-length human p53 protein. *Biochemistry 40*, 3847-3858.

(12) Bell, S., Klein, C., Muller, L., Hansen, S., and Buchner, J. (2002) p53 contains large unstructured regions in its native state. *J Mol Biol 322*, 917-927.

(13) Kussie, P. H., Gorina, S., Marechal, V., Elenbaas, B., Moreau, J., Levine, A. J., and Pavletich, N. P. (1996) Structure of the MDM2 oncoprotein bound to the p53 tumor suppressor transactivation domain. *Science 274*, 948-953.

(14) Nichols, N. M., and Matthews, K. S. (2002) Human p53 phosphorylation mimic, S392E, increases nonspecific DNA affinity and thermal stability. *Biochemistry 41*, 170-178.

(15) Sakaguchi, K., Sakamoto, H., Lewis, M. S., Anderson, C. W., Erickson, J. W., Appella, E., and Xie, D. (1997) Phosphorylation of serine 392 stabilizes the tetramer formation of tumor suppressor protein p53. *Biochemistry 36*, 10117-10124.
(16) Vijgenboom, E., Busch, J. E., and Canters, G. W. (1997) In vivo studies disprove an obligatory role of azurin in denitrification in Pseudomonas aeruginosa and show that azu expression is under control of rpoS and ANR. *Microbiology 143*, 2853-2863.
(17) Nar, H., Messerschmidt, A., Huber, R., van de Kamp, M., and Canters, G. W. (1992) Crystal structure of Pseudomonas aeruginosa apo-azurin at 1.85 A resolution. *FEBS Lett 306*, 119-124.
(18) Nar, H., Messerschmidt, A., Huber, R., van de Kamp, M., and Canters, G. W. (1991) Crystal structure analysis of oxidized Pseudomonas aeruginosa azurin at pH 5.5 and pH 9.0. A pH-induced conformational transition involves a peptide bond flip. *J Mol Biol 221*, 765-772.
(19) Pozdnyakova, I., Guidry, J., and Wittung-Stafshede, P. (2000) Copper triggered b-hairpin formation. Initiation site for azurin folding? *J AM Chem Soc 122*, 6337-6338.
(20) Pozdnyakova, I., Guidry, J., and Wittung-Stafshede, P. (2001) Probing copper ligands in denatured Pseudomonas aeruginosa azurin: Unfolding His117Gly and His46Gly mutants. *J Biol Inorg Chem 6*, 182-188.
(21) Pozdnyakova, I., Guidry, J., and Wittung-Stafshede, P. (2001) Copper Stabilizes Azurin by Decreasing the Unfolding Rate. *Arch. Biochem. Biophys. 390*, 146-148.
(22) Pozdnyakova, I., Guidry, J., and Wittung-Stafshede, P. (2002) Studies of Pseudomonas aeruginosa azurin mutants: cavities in beta-barrel do not affect refolding speed. *Biophysical Journal 82*, 2645-2651.
(23) Pozdnyakova, I., and Wittung-Stafshede, P. (2001) Biological relevance of metal binding before protein folding. *J Am Chem Soc 123*, 10135-10136.
(24) Pozdnyakova, I., and Wittung-Stafshede, P. (2001) Copper binding before polypeptide folding speeds up formation of active (holo) Pseudomonas aeruginosa azurin. *Biochemistry 40*, 13728-13733.
(25) Pozdnyakova, I., and Wittung-Stafshede, P. (2003) Approaching the speed limit for Greek Key beta-barrel formation: transition-state movement tunes folding rate of zinc-substituted azurin. *Biochim Biophys Acta 1651*, 1-4.
(26) Fuentes, L., Oyola, J., Fernandez, M., and Quinones, E. (2004) Conformational changes in azurin from Pseudomona aeruginosa induced through chemical and physical protocols. *Biophys J 87*, 1873-1880.
(27) Wilson, C. J., and Wittung-Stafshede, P. (2005) Role of structural determinants in folding of the sandwich-like protein Pseudomonas aeruginosa azurin. *Proc Natl Acad Sci U S A 102*, 3984-3987.
(28) Apiyo, D., and Wittung-Stafshede, P. (2005) Unique complex between bacterial azurin and tumor-suppressor protein p53. *Biochem Biophys Res Commun 332*, 965-968.
(29) Nichols, N. M., and Matthews, K. S. (2001) p53 unfolding detected by CD but not by tryptophan fluorescence. *Biochem Biophys Res Commun 288*, 111-115.
(30) Gilardi, G., Mei, G., Rosato, N., Canters, G. W., and Finazzi-Agro, A. (1994) Unique environment of Trp48 in Pseudomonas aeruginosa azurin as probed by site-

directed mutagenesis and dynamic fluorescence spectroscopy. *Biochemistry 33*, 1425-1432.

(31) Leckner, J., Wittung, P., Bonander, N., Karlsson, G., and Malmstrom, B. (1997) The effect of redox state on the folding free energy of azurin. *J. Biol. Inorg. Chem. 2*, 368-371.

(32) Bellamine, A., Mangla, A. T., Nes, W. D., and Waterman, M. R. (1999) Characterization and catalytic properties of the sterol 14alpha- demethylase from Mycobacterium tuberculosis. *Proc Natl Acad Sci U S A 96*, 8937-8942.

(33) Van Pouderoyen, G., Mazumdar, S., Hunt, N. I., Hill, A. O., and Canters, G. W. (1994) The introduction of a negative charge into the hydrophobic patch of Pseudomonas aeruginosa azurin affects the electron self-exchange rate and the electrochemistry. *Eur J Biochem 222*, 583-588.

(34) Sedlak, E., and Wittung-Stafshede, P. (2007) Discrete Roles of Copper Ions in Chemical Unfolding of Human Ceruloplasmin. *Biochemistry*.

(35) Hussain, F., Sedlak, E, Wittung-Stafshede, P. (2007) Impact of Cofactor on Stability of Bacterial (CopZ) and Human (Atox1) Copper Chaperones. *Biochim Biophys Acta*.

(36) Wadia, J. S., Stan, R. V., and Dowdy, S. F. (2004) Transducible TAT-HA fusogenic peptide enhances escape of TAT-fusion proteins after lipid raft macropinocytosis. *Nat Med 10*, 310-315.

(37) Snyder, E. L., and Dowdy, S. F. (2004) Cell penetrating peptides in drug delivery. *Pharm Res 21*, 389-393.

(38) Wadia, J. S., and Dowdy, S. F. (2005) Transmembrane delivery of protein and peptide drugs by TAT-mediated transduction in the treatment of cancer. *Adv Drug Deliv Rev 57*, 579-596.

(39) Marks, J., Pozdnyakova, I., Guidry, J., and Wittung-Stafshede, P. (2004) Methionine-121 coordination determines metal specificity in unfolded Pseudomonas aeruginosa azurin. *J Biol Inorg Chem 9*, 281-288.

Appendix

Two recently accepted papers that acknowledge support from this grant are included in this section:

1. Sedlak, E. Wittung-Stafshede, P.
Discrete Roles of Copper Ions in Chemical Unfolding of Human Ceruloplasmin
Biochemistry, in press (web publication July 28) 2007.

2. Hussain, F, Wittung-Stafshede, P.
Impact of Cofactor on Stability of Bacterial (CopZ) and Human (Atox1) Copper Chaperones
BBA - Proteins and Proteomics, in press, 2007.

Discrete Roles of Copper Ions in Chemical Unfolding of Human Ceruloplasmin†

Erik Sedlak‡,§ and Pernilla Wittung-Stafshede*,‡,||,⊥

Department of Biochemistry and Cell Biology, Keck Center for Structural Computational Biology, and Department of Chemistry, Rice University, 6100 Main Street, Houston, Texas 77251

Received April 16, 2007; Revised Manuscript Received June 25, 2007

ABSTRACT: Human ceruloplasmin (CP) is a multicopper oxidase essential for normal iron homeostasis. The protein has six β-barrel domains with one type 1 copper in each of domains 2, 4, and 6; the remaining copper ions form a catalytic trinuclear cluster, one type 2 and two type 3 coppers, at the interface between domains 1 and 6. We have characterized urea-induced unfolding of holo- and apo-forms of CP by far-UV circular dichroism, intrinsic fluorescence, 8-anilinonaphthalene-1-sulfonic acid binding, visible absorption, copper content, and oxidase activity probes (pH 7, 23 °C). We find that holo-CP unfolds in a complex reaction with at least one intermediate. The formation of the intermediate correlates with decreased secondary structure, exposure of aromatics, loss of two coppers, and reduced oxidase activity; this step is reversible, indicating that the trinuclear cluster remains intact. Further additions of urea trigger complete protein unfolding and loss of all coppers. Attempts to refold this species result in an inactive apoprotein with molten-globule characteristics. The apo-form of CP also unfolds in a multistep reaction, albeit the intermediate appears at a slightly lower urea concentration. Again, correct refolding is possible from the intermediate but not the unfolded state. Our study demonstrates that in vitro equilibrium unfolding of CP involves intermediates and that the copper ions are removed in stages. When the catalytic site is finally destroyed, refolding is not possible at neutral pH. This implies a mechanistic role for the trinuclear metal cluster as a nucleation point, aligning domains 1 and 6, during CP folding in vivo.

Ceruloplasmin (CP; EC 1.16.3.1)[1] is a circulating copper protein found in vertebrate plasma, which belongs to the family of multicopper oxidases together with ascorbate oxidase and laccases (*1*−*4*). In humans, CP accounts for ∼95% of the plasma copper and plays an important role in iron metabolism due to its ability to oxidize Fe^{2+} to Fe^{3+}, which allows for subsequent incorporation of Fe^{3+} into apotransferrin (*5*−*8*). CP is also believed to function as an antioxidant agent to scavenge free radicals, as an amine oxidase to control levels of biogenic amines, and as a copper transporter to deliver copper to extrahepatic tissues (*8*−*10*). CP is synthesized in hepatocytes and secreted into the plasma after incorporation of six copper ions in the secretory pathway (*5*). Failure to incorporate this metal during biosynthesis results in the secretion of an unstable polypeptide that is rapidly degraded in the plasma (*11*).

CP consists of a 1046 residue polypeptide and six integral copper ions classified into five different sites (*6*, *9*). The crystal structure of CP (*6*, *9*) demonstrates that the polypeptide is folded in six β-barrel domains arranged in three pairs forming a triangular array around a pseudo 3-fold axis (Figure 1). Three copper ions are found in type 1 (T1) mononuclear centers located in domains 2, 4, and 6. Copper in domains 4 (T1B) and 6 (T1A) is coordinated by two His, one Cys, and one Met, whereas the Met is absent in the metal-binding site in domain 2 (T1C) (*6*, *9*). The high reduction potential of the T1C copper indicates that it is permanently reduced and not catalytically relevant (*12*, *13*). The absorption at 610 nm that gives CP its intense blue color is a result of the oxidized coppers T1A and T1B. The remaining three coppers form a trinuclear cluster at the interface of domains 1 and 6. This cluster consists of a mononuclear type 2 (T2) and a binuclear type 3 (T3) copper site. It is envisaged that electrons are donated by substrates

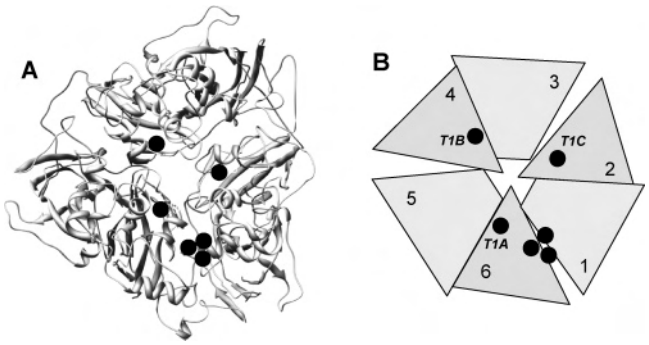

FIGURE 1: (A) Crystal structure of human CP (1kcw, pdb) with highlighted copper ions (circles) bound to the protein (UCSF Chimera). (B) Scheme of holo-CP showing the positions of the coppers (circles) in the six domains. The T1 coppers in domains 2, 4, and 6 are designated as T1C, T1B, and T1A, respectively.

† This work was funded by grants from the Robert A. Welch Foundation (C-1588) and the USAMRAA (Concept award; W81XWH-06-1-0572).

* To whom correspondence should be addressed. Tel: 713-348-4076. Fax: 713-348-5154. E-mail: pernilla@rice.edu.

‡ Department of Biochemistry and Cell Biology.

§ Permanent address: Department of Biochemistry, P.J. Safarik University, Moyzesova 11, 04001 Kosice, Slovakia.

|| Keck Center for Structural Computational Biology.

⊥ Department of Chemistry.

[1] Abbreviations: CP, ceruloplasmin; CD, circular dichroism, ANS, 8-anilinonaphthalene-1-sulfonic acid; CN, cyanide.

10.1021/bi700715e CCC: $37.00
Published on Web 07/28/2007 PAGE EST: 6.9

to T1A or T1B via outer-sphere electron transfer and then transferred to dioxygen at the trinuclear cluster (*6*, *9*, *13*−*15*). The trinuclear cluster is surrounded by four pairs of His residues equally contributed by domains 1 and 6.

Previous studies have indicated that the conformation of apo-CP has molten-globulelike properties (*16*, *17*). For more than 40 years, it has been assumed that apo-CP binds copper in an all-or-none fashion (*18*). In support, recent metabolic-labeling experiments indicated that achieving the final state of CP required occupation of all six copper-binding sites without apparent hierarchy for incorporation at any given site (*5*). On the other hand, there have also been reports that invoke the possibility of partially metallated forms of CP (*19*, *20*). On the basis of cyanide (CN)-dependent metal-removal attempts, it was suggested that the T1 coppers are more sensitive than the T2 and T3 coppers to elimination (*20*, *21*). To probe the role of the coppers in the folding mechanism of human CP, we here compare the chemically induced unfolding reactions of holo- and apo-forms using a set of biophysical tools (pH 7, 23 °C). Our study demonstrates that in vitro unfolding of both CP forms involves populated intermediates; for the holo-form, the partially folded intermediate has lost two coppers and some blue color, but the trinuclear copper cluster remains intact. It appears that this species, and thus early incorporation of the T2 and T3 copper ions, is a necessary requirement for successful in vivo biosynthesis of holo-CP.

MATERIALS AND METHODS

Chemicals and Instruments. Analytical-grade chemicals and *o*-dianisidine were obtained from Sigma-Aldrich. 2,2′-Biquinoline was obtained from Fluka. Human CP (>96% purity, $A_{610}/A_{280} = 0.046$) was obtained from Vital Products (Florida). The concentration of holo- and apo-CP was determined by ϵ_{280nm} of 200 mM^{-1} cm^{-1}. The urea concentration was determined from refractive index measurements. Absorbance, fluorescence, and far-UV circular dichroism (CD) measurements were performed on Varian Cary 50, Cary Eclipse, and Jasco J-810 spectrometers, respectively.

Copper Removal. To prepare apo-CP, 10 mg/mL of CP was dialyzed for 2 h at 23 °C against 30 mM ascorbate in 0.1 M Trizma, pH 7.2. Subsequently, dialysis continued for 20 h at 4 °C against 50 mM NaCN, 10 mM EDTA, and 10 mM ascorbate in 0.1 M Trizma, pH 7.2. The dialysis proceeded for another 24 h at 4 °C (with buffer exchange after 12 h) against 50 mM sodium phosphate buffer, pH 7.0. Alternatively, a more harsh method to prepare apo-CP involved denaturation of holo-CP in 9 M urea with subsequent dialysis against 50 mM phosphate buffer, pH 7.0, to remove the urea and dissociated coppers. The copper content to confirm 100% holo-form, and to reveal loss of copper at different urea concentrations during holo-CP unfolding, was determined according to the method developed by Felsenfeld (*22*).

Unfolding and Refolding Experiments. Samples for unfolding were prepared by suitable mixing of phosphate buffer and urea solution (9.3 M urea in 50 mM phosphate, pH 7.0) and protein (protein solution in phosphate buffer) with a final protein concentration of 2−3 μM. Samples were incubated for 1 h at 23 °C. CD was obtained from the averaged signal at 220 nm collected for 120 s at 23 °C. The same samples were used for determination of the dependence of protein fluorescence on urea concentration. Excitation was at 295 nm, and both intensity and position of emission maximum were determined from spectra obtained by averaging five consecutive scans. The same parameters characterizing 8-anilinonaphthalene-1-sulfonic acid (ANS) fluorescence were obtained from averaged emission spectra (five scans) of protein/urea samples including 200 μM ANS (excitation at 390 nm). To test for reversibility, the protein was incubated in 5.5 or 9.0 M urea, dependent on whether the first or second transition was the target, respectively. The perturbed protein was then mixed with buffer solutions containing the desired (lower) concentration of urea, and spectroscopic measurements were performed as described above. All experiments were performed at 23 °C. Each individual unfolding/refolding transition was analyzed as described in refs *23* and *24* using standard two-state equations that reveal free energies of unfolding in buffer (i.e., ΔG_U) and *m* values [i.e., a measure of cooperativity of the transition or relative exposure of the hydrophobic surface upon unfolding (*23*−*25*)].

CP Oxidase Activity Assay. The oxidase activity of CP was performed by using *o*-dianisidine (an aromatic diamine) as a substrate in accordance with the procedure by Schosinsky et al. (*26*).

Analysis of Far-UV CD Spectra. Far-UV CD spectra (190−260 nm) were recorded at 23 °C; all spectra were averages of 10 scans. Several algorithms available in DICHROWEB (*27*, *28*) were used to analyze the data. The goodness of the fits was based on the NRMSD parameter (*29*), and the best score was provided by CDSSTR (*30*).

RESULTS

Preparing Holo- and Apo-Forms of CP. Our holo-CP stocks were highly pure but sometimes (depending on storage time) contained a fraction of partially metallated protein. The oxidized T1 coppers can be identified from the 610 nm absorption. The T2 and T3 copper sites form the catalytic cluster and thus are probed indirectly via CP oxidase activity. The total number of copper ions in CP can be quantified using the 2,2′-biquinoline assay (*22*). Before each experiment, 100% holo-CP (i.e., the protein coordinating six coppers) was prepared via addition of additional copper ions in the presence of ascorbate followed by extensive dialysis to remove the excess copper (*5*). On the basis of 610 nm absorption and copper quantification, this treatment resulted in a homogeneous sample of 100% holo-CP. Different approaches to preparation of apo-CP have been described (*19*−*21*): CN dialysis under reducing conditions and high-urea treatment. Our experiments revealed that the CN dialysis method is "best" as it does not perturb the protein structure as much as urea treatment (see below). Thus, for our unfolding studies, we prepared apo-CP via CN dialysis. Metal analysis of the protein after this treatment confirmed that all copper ions had been removed.

In Figure 2, we show the far-UV CD (secondary structure) and fluorescence (tryptophan environment; CP has 19 Trp) spectra of apo- and holo-forms of CP. Secondary structure analysis of the CD data for holo-CP agree with the reported crystal structure; the signal is dominated by β-sheets, turns, and random coils, with minimal or no α-helices. Analysis of the spectra for apo-CP (prepared via CN dialysis) suggests

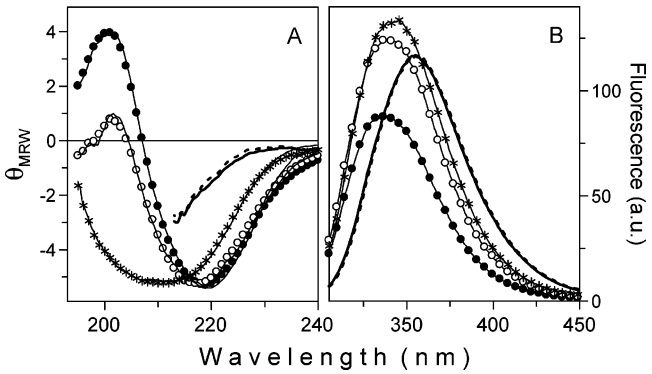

FIGURE 2: (A) Far-UV CD spectra of holo (●), apo(CN) (○), and apo(urea) (*) forms of CP. According to the CDSSTR algorithm, holo-CP contains 5% α-helix, 37% *β*-strands, 23% turns, and 33% unordered secondary structures. Corresponding contents in apo-(CN)-CP are 3% α-helix, 33% *β*-strands, 22% turns, and 41% unordered secondary structures. (B) Tryptophan emission (excitation at 295 nm) of holo (●), apo(CN) (○), and apo(urea) (*) forms of CP. For comparison, CD and fluorescence signals of fully unfolded apo- (dotted curves) and holo-CP (solid curves) (i.e., in 9 M urea) are also shown.

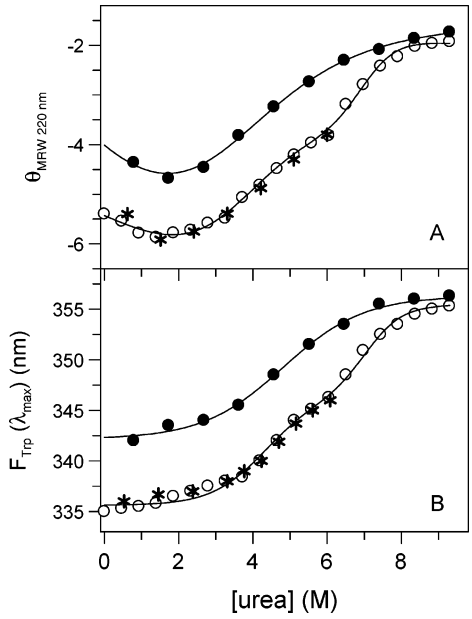

FIGURE 3: Isothermal denaturation of holo-CP followed by (A) CD at 220 nm and (B) tryptophan fluorescence (excitation at 295 nm). Unfolding of native-CP (○), refolding of CP from 5.5 M urea (*), and refolding of CP from 9.0 M urea (●). The continuous lines are fits to the experimental values (Table 1).

that the *β*-sheet content decreases with a subsequent increase in the random coil structure. Analogously, positions of maxima of tryptophan fluorescence of holo- (335 nm) and apo- (340 nm) forms indicate perturbation of the tryptophan environments in the apo-form of CP. Thus, apo-CP is structurally distinct from holo-CP: It appears to have lost some native structural elements. For comparison, CD and fluorescence spectra for fully unfolded forms are also shown in Figure 2.

Unfolding of Holo-CP. Unfolding of holo-CP was induced by urea additions at pH 7 and 23 °C. In Figure 3, we show the far-UV CD and fluorescence signals as a function of urea concentration. It is apparent that the process is not a simple two-state process but involves at least two steps. There appears to be a first transition with a midpoint of ∼4.2 M

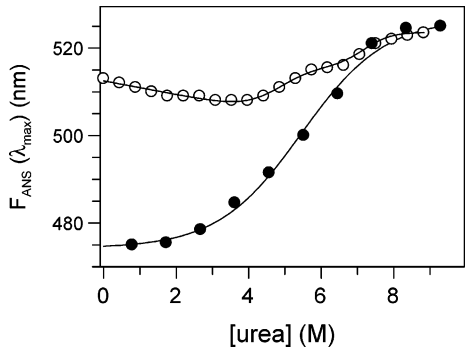

FIGURE 4: Isothermal denaturation of holo-CP followed by ANS fluorescence (excitation at 390 nm). Unfolding of native-CP (○) and refolding of CP from 9.0 M urea (●). The continuous lines are fits to experimental values (Table 1).

urea, resulting in the loss of about 30−40% of the far-UV CD intensity and a shift of the emission maximum toward higher wavelengths (i.e., from 335 to 345 nm) although the intensity does not change much. This first process is followed by a second transition that has a midpoint of ∼7.0 M urea. In this step, the fully unfolded form of the protein is reached according to the far-UV CD and tryptophan emission maximum (now at 355 nm) and intensity changes.

The unfolding reaction of holo-CP induced by urea was also probed via ANS emission (Figure 4). ANS is a fluorophore that emits strongly around 500 nm when bound to hydrophobic surfaces and pockets; it is often used as a tool to detect intermediate species of proteins as it does not significantly bind to either folded or unfolded forms (*31*, *32*). We find that the ANS emission shifts in a biphasic way that matches the two transitions observed for holo-CP with far-UV CD and tryptophan fluorescence. First, there is a small increase in the ANS emission together with a shift of the peak toward a higher maximum wavelength: This transition has a midpoint at ∼4−5 M urea. This change is followed by a further shift toward higher wavelengths of the ANS emission maximum in a second transition with a midpoint at ∼7 M urea. This result supports the presence of an intermediate species at intermediate urea concentrations (i.e., at ∼5.5 M urea).

The fates of the copper ions during urea treatment were tested by visible absorption at 610 nm (probing the oxidized T1 sites), copper analysis (probing total copper content), and oxidase activity (probing the catalytic cluster) as a function of urea (Figure 5). We find ∼50% decrease of 610 nm absorbance (which may correspond to destruction of one of the two oxidized T1 sites) in a first phase that parallels the first CD/fluorescence-detected transition. Copper quantification revealed that in total two copper ions have been removed from the protein at 5.5 M urea. The remaining blue color disappears at higher urea concentrations (6−7 M urea) together with loss of all copper ions (Figure 5). CP's oxidase activity disappears in a three-state transition that matches the disappearance of blue absorption (Figure 5): The first process results in a loss of about 60% activity. This indicates that although the intermediate form of CP at 5.5 M urea has lost some coppers, the catalytic copper cluster is still functional.

The binding site of aromatic diamine substrates such as *o*-dianisidine used here is located in domain 4 near T1B (*6*); thus, if this is the perturbed oxidized T1 site in the

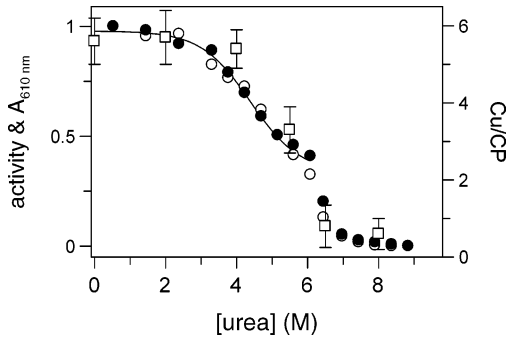

FIGURE 5: Isothermal denaturation of holo-CP followed by oxidase activity (○) monitored by reaction of CP with *o*-dianisidine and by visible absorbance at 610 nm (●). The total copper content in CP at different urea concentrations are also shown. The amount of copper (□) was quantified after dialysis of samples at each specified urea concentration, to remove any dissociated copper ions. The continuous lines are fits to experimental values (Table 1).

intermediate, one may expect less activity. However, also, removal of T1A may affect electron transfer from T1B to the catalytic cluster. On the basis of our data, we cannot distinguish which oxidized T1 site is perturbed. The T1C copper is spectrally invisible as it is permanently reduced (*13*). It is probable that this copper ion, missing one protein ligand as compared to the other T1 sites, will dissociate most readily of all copper cofactors in CP. Thus, it appears reasonable that this copper is one of the two metals removed in the intermediate. We note that the tryptophan fluorescence in folded holo-CP is quenched by the metals; in accord with several metals remaining in the intermediate, the emission stays quenched until ~7 M urea has been added (data not shown).

Next, refolding of holo-CP from the intermediate (i.e., 5.5 M urea) and fully unfolded (i.e., 9 M urea) states was tested. We find that nativelike far-UV CD and Trp fluorescence signals appear upon refolding from the intermediate species (Figure 3). Also, the blue color and oxidase activity return to native-state levels when refolded from the 5.5 M urea state. This suggests that albeit two coppers are gone in the intermediate, these can rebind upon protein refolding.

In contrast, refolding from the unfolded state (9 M urea) results in a protein species distinctly different from the native state. This form has an intermediate-sized far-UV CD signal (and different shape), only partial restoration of the native-like tryptophan emission, no blue color, no copper bound, no oxidase activity, and is found to interact strongly with ANS (Figures 3 and 4). For this species, the ANS emission is increased 3-fold as compared to that for the native-state and 2-fold as compared to that for the intermediate and unfolded states; moreover, the emission maximum is largely red-shifted to 480 nm. Taken together, these properties are indicative of a molten-globulelike species (*33*−*38*). Refolding into the molten-globule species occurs in a broad transition with a midpoint of 4.0−4.5 M urea. Repeated unfolding reveals the same urea-unfolding curve as the one obtained in the refolding experiments from 9 M urea, in accord with reversibility (data not shown). On the basis of the spectroscopic properties, the molten-globulelike CP form is not identical to the apo-form that is prepared via CN dialysis (see below).

The parameters obtained from fits to the different holo-CP unfolding curves are reported in Table 1. It is clear that

Table 1: Parameters Describing the Conformational Transitions of Holo- and Apo-CP as Monitored by Far-UV CD (CD_{220} nm), Tryptophan (F_{Trp}), and ANS (F_{ANS}) Fluorescence Maxima Placement, Blue Copper Absorbance (A_{610} nm), and Oxidase Activity[a]

detection	urea change (M)	ΔG_U (kJ/mol)	*m* (kJ/mol, M)	$[urea]_{1/2}$ (M)
		holo-form		
CD_{220nm}	0 → 5.5	15.3 ± 0.7	3.7 ± 0.2	4.1
CD_{220nm}	5.5 → 9	39.5 ± 3.0	5.7 ± 0.4	6.9
CD_{220nm}	5.5 → 0	−15.2 ± 1.1	3.6 ± 0.3	4.3
CD_{220nm}	9 → 0	−8.6 ± 0.9	1.9 ± 0.2	4.6
F_{Trp}	0 → 5.5	15.2 ± 1.3	3.5 ± 0.2	4.3
F_{Trp}	5.5 → 9	37.4 ± 2.0	5.3 ± 0.4	7.0
F_{Trp}	5.5 → 0	−17.1 ± 1.5	3.8 ± 0.3	4.5
F_{Trp}	9 → 0	−10.9 ± 1.0	2.3 ± 0.2	4.2
F_{ANS}	0 → 5.5			5.0
F_{ANS}	5.5 → 9			7.1
F_{ANS}	9 → 0	−11.7 ± 1.2	2.1 ± 0.2	5.4
activity	0 → 5.5	15.6 ± 1.9	3.6 ± 0.4	4.4
A_{610nm}	0 → 5.5	17.2 ± 1.2	4.1 ± 0.3	4.2
		apo-form		
CD_{220nm}	0 → 5.5	14.4 ± 1.1	3.1 ± 0.3	3.8
CD_{220nm}	5.5 → 9	36.5 ± 3.9	4.8 ± 0.5	7.6
CD_{220nm}	5.5 → 0	−13.2 ± 1.1	3.6 ± 0.3	3.7
F_{Trp}	0 → 5.5	14.6 ± 0.7	4.2 ± 0.2	3.5
F_{Trp}	5.5 → 9	28.8 ± 2.0	4.5 ± 0.3	6.4
F_{Trp}	5.5 → 0	−12.5 ± 3.7	3.7 ± 0.7	3.4
F_{ANS}	0 → 5.5	13.6 ± 1.5	2.9 ± 0.3	4.6

[a] The direction of the urea jump (i.e., unfolding or refolding) is indicated. ΔG_U, *m* values, and $[urea]_{1/2}$ were obtained from two-state fits to individual transitions. (Fit parameters for most of the ANS data were not reliable and are not shown.)

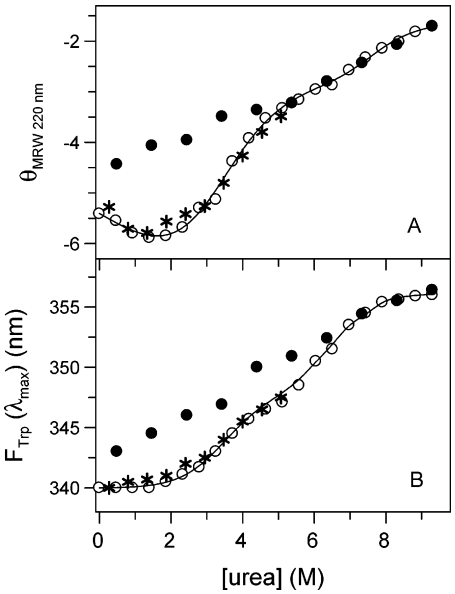

FIGURE 6: Isothermal denaturation of apo-CP followed by (A) CD at 220 nm and (B) tryptophan fluorescence (excitation at 295 nm). Unfolding of native-CP (○), refolding of CP from 5.5 M urea (*), and refolding of CP from 9.0 M urea (●). The continuous lines are fits to experimental values (Table 1).

the parameters for the first transition, from native to intermediate state, match among the five detection methods and correspond to a free-energy change of about 15 kJ/mol (pH 7, 23 °C). The *m* value, indicative of relative exposure of hydrophobic surfaces upon perturbation (*23*−*25*), is low for the protein of this size (120 kDa), supporting that only partial unfolding is involved in the transition. The second

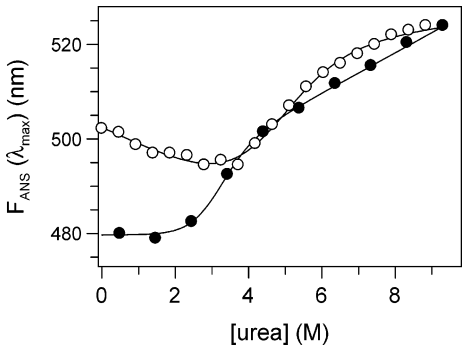

FIGURE 7: Isothermal denaturation of apo-CP followed by ANS fluorescence (excitation at 390 nm). Unfolding of native-CP (○) and refolding of CP from 9.0 M urea (●). The continuous lines are fits to experimental values (Table 1).

step, intermediate to unfolded, is irreversible, and one must use caution when analyzing the fit parameters. Nonetheless, it appears that this transition involves a higher free-energy change and more hydrophobic surface exposure than the first process. The refolding/unfolding of the molten-globule species, which is a reversible transition, corresponds to a free-energy change of about 10 kJ/mol (pH 7, 23 °C) and low cooperativity based on the low *m* value.

Unfolding Apo-CP. Urea-induced unfolding was also investigated with apo-CP prepared by CN dialysis. In Figure 6, far-UV CD and fluorescence curves as a function of urea concentration are shown. Again, unfolding appears in two phases, a first transition with a midpoint of about 3.5 M urea followed by a second transition with a midpoint of about 6−7 M urea. The intermediate species has only ~35% of the original negative far-UV CD signal; the emission maximum is shifted from 340 to 347 nm. ANS binding to apo-CP vs urea concentration was also tested; the results mimic the trends seen above for the holo-protein (Figure 7); again, a biphasic transition is observed when the ANS emission maximum is plotted vs urea concentration.

Whereas refolding of the intermediate species (from 5.5 M urea) results in an apo-protein that is identical to that of the starting form, refolding from 9 M urea again results in the molten-globulelike species that has distinct CD/fluorescence and ANS-binding properties (Figures 6 and 7). As in the case of the fully unfolded holo-protein, refolding of the apo-protein from 9 M urea occurs in a broad transition with a midpoint of ~4.3 M urea. Fits to the different apo-protein unfolding curves are listed in Table 1.

DISCUSSION

The majority of cuproenzymes, including blood-clotting factors, tyrosinase, lysyl oxidase, and CP, are synthesized within the secretory pathway (*39*); copper gains access to this compartment via copper-translocating ATPases present in the *trans*-Golgi membrane (*39*−*41*). Copper incorporation into polypeptides inside this compartment is not clear; it has been proposed that copper ions and proteins meet in vesicular environments before secretion (*5*, *8*). As a first step toward elucidating the interplay between copper uptake and polypeptide folding of cuproproteins made in the secretory pathway, we have characterized the in vitro chemical unfolding reactions of purified apo- and holo-forms of human CP.

Both forms of CP are found to unfold in multistep equilibrium reactions, involving at least one on-pathway intermediate and one misfolded off-pathway species. The

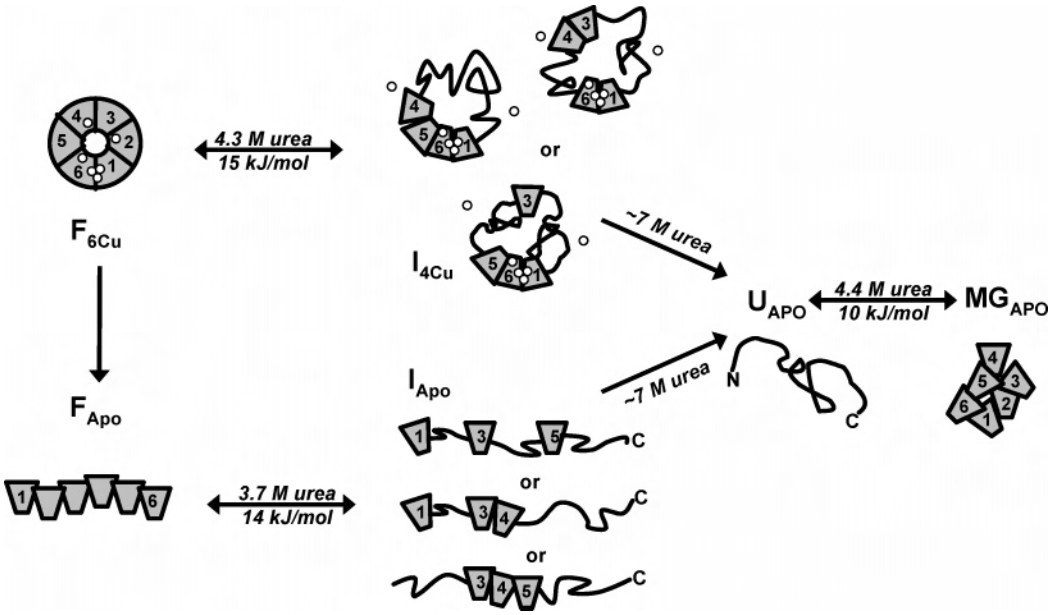

FIGURE 8: Unfolding/refolding pathways of holo- and apo-CP based on the present work. Folded holo-CP containing six bound coppers (circles), F_{6Cu}, undergoes a reversible transition up to ~5.5 M urea, with a midpoint at ~4.3 M, losing two copper ions and about half of the oxidase activity and blue absorption. This intermediate form of holo-CP is termed I_{4Cu}. This intermediate may have T1C and T1B coppers removed (see text) and two domains unfolded, perhaps involving those harboring the destroyed copper sites; the catalytic cluster and therefore domains 1 and 6 are likely intact in the intermediate. Three possible structures of I_{4Cu} are shown. A further increase in urea concentration leads to full CP unfolding accompanied by dissociation of all coppers, U_{Apo}. Analogously, F_{Apo} (prepared via CN dialysis) undergoes a reversible urea-induced transition with a midpoint at ~3.7 M (forming I_{Apo}; three possible structures are shown), followed by an irreversible transition to U_{Apo} completed at 9.3 M urea. The final unfolded state of apo-CP is similar to that obtained when starting from holo-CP. U_{Apo} undergoes a reversible off-pathway transition to a molten globulelike state, MG_{Apo}, with a midpoint at 4.4 M urea. Double-headed arrows indicate reversibility; single-headed arrows depict transitions that only go in one direction. Midpoints and stabilities are from Table 1.

proposed folding/unfolding landscape for holo- and apo-forms of CP (i.e., F_{6Cu} and F_{apo}) in urea (pH 7, 23 °C), and tentative structural aspects of the intermediates, are summarized in Figure 8. First, the activity data suggest that the holo-intermediate (i.e., I_{4Cu}) has an intact trinuclear copper cluster; thus, the interface between domains 1 and 6 where this site is located is likely intact; therefore, domains 1 and 6 remain folded. Because the holo-intermediate has lost about 30−40% of its secondary structure (which equals two out of six domains) and two coppers, one being an oxidized T1 copper (based on the blue color change), it is possible that domains 2 (containing silent T1C) and 4 (containing T1B) are unfolded in I_{4Cu}. Notably, the disulfide bonds in domains 2 and 4 link different β-strands as compared to the disulfide bonds in domains 1, 3, and 5 (*6*, *9*); this may account for differential domain stability. Earlier work (*19*) gives support that T1B, and not T1A, is the oxidized T1 copper removed in the unfolding intermediate. It was reported that upon loss of two coppers via CN dialysis, CP lost half of its blue color and most of its oxidase activity (substrate binding near T1B) disappeared whereas most of the dismutase activity (substrate binding near T1A) remained (*19*). That a few domains are unfolded and a few remain folded is in agreement with the ANS data, which do not indicate that the whole protein is partially folded [if so, we would observe a dramatic increase in ANS emission and a red shift of its maximum (*25*)]. Further additions of urea result in complete polypeptide unfolding and loss of all coppers (i.e., U_{apo}).

The apo-form of CP (i.e., F_{apo}) has been proposed to adopt a folded but extended form in which the interface between domains 1 and 6 is absent (*21*); the domains may be depicted as beads on a string with domain 1 spatially distant from domain 6. Conversion of apo-CP to the intermediate state (i.e., I_{apo}) again appears to involve selective unfolding of some of the domains based on the spectroscopic signals. Further perturbation of the apo-intermediate results in a fully unfolded state with all domains unfolded (i.e., U_{apo}). Refolding of U_{apo} (obtained from complete unfolding of both holo- and apo-forms of CP) occurs, reversibly, into an off-pathway copper-lacking molten globule (i.e., MG_{apo}). This form may have several domains folded, as it has a significant secondary structure content, but the arrangement of the domains in three-dimensional space, and interdomain interactions, may be incorrect, prohibiting copper incorporation and proper folding.

Several biological implications can be drawn from our findings. First, it is clear that, in contrast to small proteins where bound cofactors often have large effects on protein stability (*42*−*49*), the coppers in CP contribute minimally to the overall protein stability. The transition midpoints are found at roughly the same urea concentrations for both apo- and holo-forms (Table 1). Furthermore, because apo-CP may have a more extended conformation, it appears that the individual domains, and not the domain−domain interactions, govern most of the protein's stability. Second, our experiments suggest a mechanistic role for the trinuclear copper cluster in proper alignment of domains 1 and 6; only when this interface/metal site is in place is correct CP folding possible in our experiments. In agreement, several demetalation studies have demonstrated that if all six coppers are removed from CP, reconstitution is not possible at neutral and oxidizing conditions (*19*, *21*). Reconstitution of apo-CP has only been achieved in some special conditions, that is, in the presence of ascorbate at pH 5.6 and only partially via Cu(I)-glutathione in the presence of Mg-ATP at pH 7 (*5*, *17*, *50*). Third, our findings provide mechanistic insight into the recently proposed CP biosynthesis pathway (*5*). It was demonstrated via metabolic labeling and gel shift experiments that copper incorporation into CP is an all-or-none process, although the possibility of unstable, "hidden" intermediates was mentioned (*5*). We propose that the intermediate detected here with an intact trinuclear copper site is such a hidden intermediate not resolved by the methods used in ref *5*. This intermediate may form for several of the copper-site mutants studied in ref *5*, but their low stability causes them to return to the apo-form if the remaining T1 copper ions are not incorporated (due to mutations of copper ligands).

Finally, our study implies that the CP polypeptide can adopt a molten-globule form that is not on the path to the native state. Thus, timely copper incorporation, before apoprotein misfolding occurs, may be crucial for successful in vivo biosynthesis of CP. Notably, we have earlier shown that for *Pseudomonas aeruginosa* azurin, copper binding readily occurs in the unfolded state (*51*, *52*). Additional studies using strategic CP mutants and solvent conditions mimicking the biological environment in the secretory pathway will be of importance from a fundamental point of view, as it may apply to other cuproproteins made in the secretory pathway, and also from a medical aspect, as it may facilitate new approaches to incorporate copper into copper-lacking CP variants found in affected patients.

REFERENCES

1. Holmberg, C. G., and Laurell, C. B. (1948) Investigations in serum copper II: Isolation of the copper-containing protein and a description of some of its properties, *Acta Physiol. Scand. 2*, 550−556.
2. Palmer, A. E., Quintanar, L., Severance, S., Wang, T. P., Kosman, D. J., and Solomon, E. I. (2002) Spectroscopic characterization and O2 reactivity of the trinuclear Cu cluster of mutants of the multicopper oxidase Fet3p, *Biochemistry 41*, 6438−6448.
3. Quintanar, L., Gebhard, M., Wang, T. P., Kosman, D. J., and Solomon, E. I. (2004) Ferrous binding to the multicopper oxidases Saccharomyces cerevisiae Fet3p and human ceruloplasmin: Contributions to ferroxidase activity, *J. Am. Chem. Soc. 126*, 6579−6589.
4. Wang, T. P., Quintanar, L., Severance, S., Solomon, E. I., and Kosman, D. J. (2003) Targeted suppression of the ferroxidase and iron trafficking activities of the multicopper oxidase Fet3p from Saccharomyces cerevisiae, *J. Biol. Inorg. Chem. 8*, 611−620.
5. Hellman, N. E., Kono, S., Mancini, G. M., Hoogeboom, A. J., De Jong, G. J., and Gitlin, J. D. (2002) Mechanisms of copper incorporation into human ceruloplasmin, *J. Biol. Chem. 277*, 46632−46638.
6. Zaitsev, V. N., Zaitseva, I., Papiz, M., and Lindley, P. F. (1999) An X-ray crystallographic study of the binding sites of the azide inhibitor and organic substrates to ceruloplasmin, a multi-copper oxidase in the plasma, *J. Biol. Inorg. Chem. 4*, 579−587.
7. Osaki, S., Johnson, D. A., and Frieden, E. (1966) The possible significance of the ferrous oxidase activity of ceruloplasmin in normal human serum, *J. Biol. Chem. 241*, 2746−2751.
8. Hellman, N. E., and Gitlin, J. D. (2002) Ceruloplasmin metabolism and function, *Annu. Rev. Nutr. 22*, 439−458.
9. Lindley, P. F. (2001) Ceruloplasmin, *Handb. Metalloproteins*, 1369−1380.
10. Musci, G., Bellenchi, G. C., and Calabrese, L. (1999) The multifunctional oxidase activity of ceruloplasmin as revealed by anion binding studies, *Eur. J. Biochem. 265*, 589−597.
11. Gitlin, J. D., Schroeder, J. J., Lee-Ambrose, L. M., and Cousins, R. J. (1992) Mechanisms of caeruloplasmin biosynthesis in normal and copper-deficient rats, *Biochem. J. 282* (Part 3), 835−839.

12. Machonkin, T. E., Zhang, H. H., Hedman, B., Hodgson, K. O., and Solomon, E. I. (1998) Spectroscopic and magnetic studies of human ceruloplasmin: identification of a redox-inactive reduced Type 1 copper site, *Biochemistry 37*, 9570−9578.
13. Machonkin, T. E., and Solomon, E. I. (2000) The thermodynamics, kinetics and molecular mechanism of intramolecular electron transfer in human ceruloplasmin, *J. Am. Chem. Soc. 122*, 12547−12560.
14. Mukhopadhyay, C. K., Mazumder, B., Lindley, P. F., and Fox, P. L. (1997) Identification of the prooxidant site of human ceruloplasmin: A model for oxidative damage by copper bound to protein surfaces, *Proc. Natl. Acad. Sci. U.S.A. 94*, 11546−11551.
15. Calabrese, L., Carbonaro, M., and Musci, G. (1989) Presence of coupled trinuclear copper cluster in mammalian ceruloplasmin is essential for efficient electron transfer to oxygen, *J. Biol. Chem. 264*, 6183−6187.
16. De Filippis, V., Vassiliev, V. B., Beltramini, M., Fontana, A., Salvato, B., and Gaitskhoki, V. S. (1996) Evidence for the molten globule state of human apo-ceruloplasmin, *Biochim. Biophys. Acta 1297*, 119−123.
17. Sato, M., and Gitlin, J. D. (1991) Mechanisms of copper incorporation during the biosynthesis of human ceruloplasmin, *J. Biol. Chem. 266*, 5128−5134.
18. Isen, P., and Morell, A. G. (1965) Physical and chemical studies on ceruloplasmin. 3. A stabilizing copper-copper interaction in ceruloplasmin, *J. Biol. Chem. 240*, 1974−1978.
19. Vassiliev, V. B., Kachurin, A. M., Beltramini, M., Rocco, G. P., Salvato, B., and Gaitskhoki, V. S. (1997) Copper depletion/repletion of human ceruloplasmin is followed by the changes in its spectral features and functional properties, *J. Inorg. Biochem. 65*, 167−174.
20. Musci, G., Fraterrigo, T. Z., Calabrese, L., and McMillin, D. R. (1999) On the lability and functional significance of the type 1 copper pool in ceruloplasmin, *J. Biol. Inorg. Chem. 4*, 441−446.
21. Vachette, P., Dainese, E., Vasyliev, V. B., Di Muro, P., Beltramini, M., Svergun, D. I., De Filippis, V., and Salvato, B. (2002) A key structural role for active site type 3 copper ions in human ceruloplasmin, *J. Biol. Chem. 277*, 40823−40831.
22. Felsenfeld, G. (1960) The determination of cuprous ion in copper proteins, *Arch. Biochem. Biophys. 87*, 247−251.
23. Santoro, M. M., and Bolen, D. W. (1992) A test of the linear extrapolation of unfolding free energy changes over an extended denaturant concentration range, *Biochemistry 31*, 4901−4907.
24. Santoro, M. M., and Bolen, D. W. (1988) Unfolding free energy changes determined by the linear extrapolation method. 1. Unfolding of phenylmethanesulfonyl α-chymotrypsin using different denaturants, *Biochemistry 27*, 8063−8068.
25. Fersht, A. (1999) *Structure and Mechanism in Protein Science*, W. H. Freeman and Company, New York.
26. Schosinsky, K. H., Lehmann, H. P., and Beeler, M. F. (1974) Measurement of ceruloplasmin from its oxidase activity in serum by use of *o*-dianisidine dihydrochloride, *Clin. Chem. 20*, 1556−1563.
27. Lobley, A., Whitmore, L., and Wallace, B. A. (2002) DICHROWEB: An interactive website for the analysis of protein secondary structure from circular dichroism spectra, *Bioinformatics 18*, 211−212.
28. Whitmore, L., and Wallace, B. A. (2004) DICHROWEB, an online server for protein secondary structure analyses from circular dichroism spectroscopic data, *Nucleic Acids Res. 32*, W668−W673.
29. Mao, D., Wachter, E., and Wallace, B. A. (1982) Folding of the mitochondrial proton adenosinetriphosphatase proteolipid channel in phospholipid vesicles, *Biochemistry 21*, 4960−4968.
30. Manavalan, P., and Johnson, W. C., Jr. (1987) Variable selection method improves the prediction of protein secondary structure from circular dichroism spectra, *Anal. Biochem. 167*, 76−85.
31. Apiyo, D., Guidry, J., and Wittung-Stafshede, P. (2000) No cofactor effect on equilibrium unfolding of Desulfovibrio desulfuricans flavodoxin, *Biochim. Biophys. Acta 1479*, 214−224.
32. Muralidhara, B. K., and Wittung-Stafshede, P. (2005) FMN binding and unfolding of Desulfovibrio desulfuricans flavodoxin: "Hidden" intermediates at low denaturant concentrations, *Biochim. Biophys. Acta 1747*, 239−250.
33. Redfield, C., Smith, R. A., and Dobson, C. M. (1994) Structural characterization of a highly-ordered 'molten globule' at low pH, *Nat. Struct. Biol. 1*, 23−29.
34. Ptitsyn, O. (1996) How molten is the molten globule? [news], *Nat. Struct. Biol. 3*, 488−490.
35. Gast, K., Damaschun, H., Misselwitz, R., Muller-Frohne, M., Zirwer, D., and Damaschun, G. (1994) Compactness of protein molten globules: Temperature-induced structural changes of the apomyoglobin folding intermediate, *Eur. Biophys. J. 23*, 297−305.
36. Eliezer, D., and Wright, P. E. (1996) Is apomyoglobin a molten globule? Structural characterization by NMR, *J. Mol. Biol. 263*, 531−538.
37. Dobson, C. M. (1994) Protein folding. Solid evidence for molten globules, *Curr. Biol. 4*, 636−640.
38. Baum, J., Dobson, C. M., Evans, P. A., and Hanley, C. (1989) Characterization of a partly folded protein by NMR methods: Studies on the molten globule state of guinea pig alpha-lactalbumin, *Biochemistry 28*, 7−13.
39. Harris, E. D. (2003) Basic and clinical aspects of copper, *Crit. Rev. Clin. Lab. Sci. 40*, 547−586.
40. Hung, I. H., Suzuki, M., Yamaguchi, Y., Yuan, D. S., Klausner, R. D., and Gitlin, J. D. (1997) Biochemical characterization of the Wilson disease protein and functional expression in the yeast Saccharomyces cerevisiae, *J. Biol. Chem. 272*, 21461−21466.
41. Hamza, I., Schaefer, M., Klomp, L. W., and Gitlin, J. D. (1999) Interaction of the copper chaperone HAH1 with the Wilson disease protein is essential for copper homeostasis, *Proc. Natl. Acad. Sci. U.S.A. 96*, 13363−13368.
42. Wilson, C. J., Apiyo, D., and Wittung-Stafshede, P. (2004) Role of cofactors in metalloprotein folding, *Q. Rev. Biophys. 37*, 285−314.
43. Winkler, J. R., Wittung-Stafshede, P., Leckner, J., Malmstrom, B. G., and Gray, H. B. (1997) Effects of folding on metalloprotein active sites, *Proc. Natl. Acad. Sci. U.S.A. 94*, 4246−4249.
44. Wittung-Stafshede, P. (2004) Role of cofactors in folding of the blue-copper protein azurin, *Inorg. Chem. 43*, 7926−7933.
45. Goedken, E. R., Keck, J. L., Berger, J. M., and Marqusee, S. (2000) Divalent metal cofactor binding in the kinetic folding trajectory of *Escherichia coli* ribonuclease HI, *Protein Sci. 9*, 1914−1921.
46. Filimonov, V. V., Prieto, J., Martinez, J. C., Bruix, M., Mateo, P. L., and Serrano, L. (1993) Thermodynamic analysis of the chemotactic protein from *Escherichia coli*, CheY, *Biochemistry 32*, 12906−12921.
47. Bollen, Y. J., Nabuurs, S. M., van Berkel, W. J., and van Mierlo, C. P. (2005) Last in, first out: The role of cofactor binding in flavodoxin folding, *J. Biol. Chem. 280*, 7836−7844.
48. Hargrove, M. S., and Olson, J. S. (1996) The stability of holomyoglobin is determined by heme affinity, *Biochemistry 35*, 11310−11318.
49. Feng, Y. Q., and Sligar, S. G. (1991) Effect of heme binding on the structure and stability of *Escherichia coli* apocytochrome b562, *Biochemistry 30*, 10150−10155.
50. Musci, G., Di Marco, S., Bellenchi, G. C., and Calabrese, L. (1996) Reconstitution of ceruloplasmin by the Cu(I)-glutathione complex. Evidence for a role of Mg2+ and ATP, *J. Biol. Chem. 271*, 1972−1978.
51. Pozdnyakova, I., and Wittung-Stafshede, P. (2001) Biological relevance of metal binding before protein folding, *J. Am. Chem. Soc. 123*, 10135−10136.
52. Pozdnyakova, I., and Wittung-Stafshede, P. (2001) Copper binding before polypeptide folding speeds up formation of active (holo) *Pseudomonas aeruginosa* azurin, *Biochemistry 40*, 13728−13733.

BI700715E

Impact of Cofactor on Stability of Bacterial (CopZ) and Human (Atox1) Copper Chaperones

Faiza Hussain[1] and Pernilla Wittung-Stafshede[1,2,3*]

[1]*Department of Biochemistry and Cell Biology,* [2]*Department of Chemistry,* [3]*Keck Center for Structural Computational Biology, Rice University, 6100 Main Street, Houston, Texas 77251*

* *Corresponding author:* Pernilla Wittung-Stafshede, email: pernilla@rice.edu

Summary

Here, we present the first characterization of *in vitro* unfolding and thermodynamic stability of two copper chaperone proteins: *Bacillus subtilis* CopZ and *Homo sapiens* Atox1. We find that the unfolding reactions for apo- and Cu(I)-forms of CopZ and Atox1, induced by the chemical denaturant, guanidine hydrochloride (GuHCl), and by thermal perturbation are reversible two-state reactions. For both proteins, the unfolding midpoints shift to higher GuHCl concentrations and the thermodynamic stability is increased in the presence of Cu(I). Despite the same overall fold, apo-CopZ exhibits much lower thermal stability than apo-Atox1. Although the thermal stability of both proteins is increased in the presence of copper, the stabilizing effect is largest for the less stable variant. Divergent energetic properties of the apo- and holo-forms may be linked to conformational changes that facilitate copper transfer to the target.

Keywords: protein folding, metallo-chaperone, protein stability, copper metabolism, spectroscopy

Abbreviations: CD, circular dichroism; T_m, thermal midpoint; DTT, dithiothreitol

Introduction

Copper is one of the most prevalent transition metals in living organisms [1]; its biological function is intimately related to its redox properties. Many proteins that participate in cellular respiration, antioxidant defense, neurotransmitter biosynthesis, connective-tissue biosynthesis and pigment formation use copper as the prosthetic, active group [2-5]. Since free copper is toxic, copper homeostasis in living organisms is tightly controlled by subtle molecular mechanisms [6-8]. In eukaryotes, before cellular uptake via high-affinity copper transporters of the CTR family [5], Cu(II) ions are reduced to Cu(I). During the past decade, an important class of proteins, termed copper-chaperones, has been identified in the cytoplasm that binds Cu(I) with Cys_2 coordination [5, 9-12]. These small, soluble proteins guide and protect the copper ions within the cell, delivering them to the appropriate functional protein receptors. P-type ATPases are membrane spanning receptor proteins with cytoplasmic metal-binding domains that transfer Cu(I) through membranes from one cellular compartment to another. In humans, ATP7A (*i.e.*, Menkes disease protein) and ATP7B (*i.e.*, Wilson disease protein) proteins are P-type ATPases involved in copper transport [5, 10, 13]; in an ATP-dependent process, they translocate copper from the cytoplasm into the Golgi lumen for insertion into enzymes in the secretory pathway [5], such as apo-ceruloplasmin [14].

One hallmark of the copper chaperones is the similarity of the fold between the chaperone and the target metal-binding domains of the ATPases [2, 15, 16]. Solution NMR and X-ray crystal structures [15-23] demonstrate that these proteins possess a βαββαβ ferredoxin-like fold with the metal ion bound by the two cysteines in a MXCXXC motif in a surface-accessible loop towards the N-terminus (Figure 1). Despite the wealth of structural data, *there is no folding or*

stability data on copper-transport proteins. Since these proteins switch between apo- and holo-forms as part of their functional cycle, biophysical properties of both states are of biological relevance and may explain how vectorial copper transport is achieved despite an apparent shallow thermodynamic gradient [24].

To address this issue, we have compared the *in vitro* unfolding processes and thermodynamic stability of homologous copper chaperones from two different organisms: *B. subtilis* CopZ and *H. sapiens* Atox1. Although these proteins share only 15 % sequence identity, they both have the ferredoxin-like fold and the conserved copper-binding motif (Figure 1). We find that both proteins can unfold in two-state, reversible equilibrium reactions. While Atox1 is more resistant than CopZ to thermal perturbations, in both apo- and holo-forms, the difference in thermodynamic stability between the two homologs at room temperature is small. For both Atox1 and CopZ, the coordination of the Cu(I) cofactor stabilizes the folded state towards perturbations.

Materials and Methods

Protein preparation

A pALTER-Ex1 plasmid with the CopZ gene and a pET28a vector with the *H. sapiens* Atox1 gene were expressed in *E. coli*. For both proteins, published purification protocols were followed [24, 25] with slight modifications. The proteins were purified in apo-forms. Additional EDTA dialysis was employed to assure no zinc contamination. Protein molecular weights were confirmed by mass spectrometry. Protein samples were stored at -80 °C, in the presence of 1 mM DTT, until use. DTT was removed by extensive dialysis (4 buffer exchanges) to buffer without DTT under argon gas. The presence of the two cysteines in the metal-binding motif was verified with Ellman's assay on samples in the absence of DTT. In copper titrations to apo-CopZ or apo-Atox1, copper was added as $CuCl_2$ in presence/absence of 1 mM DTT as indicated. Unfolding experiments on apo- and Cu(I)-forms of the two proteins were performed in the presence of 1 mM DTT if not otherwise noted.

Spectroscopy

Far-UV CD was measured in a 1-mm cell between 200 and 300 nm; near-UV CD was measured in a 1-cm cell between 250 and 400 nm (Jasco J-810 spectropolarimeter). Tyrosine fluorescence was measured on a Varian Eclipse fluorometer with excitation at 280 nm and emission monitored between 290 and 400 nm.

Chemical and thermal unfolding

GuHCl-induced unfolding was performed in 20 mM Tris, pH 7.5, 20 °C, 1 mM DTT, 30 μM protein (apo- or holo-forms of CopZ or Atox1). To obtain the holo-forms, 1 equivalent of copper was added as $CuCl_2$; in the presence of DTT, the Cu(II) is reduced to Cu(I) [25, 26]. In some protein samples, DTT was removed before Cu(II) was added (see text). All samples were incubated for 2 hours before far-UV CD and fluorescence spectroscopic measurements. There was no time dependence in the reactions for incubation time variations from 30 min to 6 hours. Thermal CD and fluorescence data (CD signal at 220 nm and emission at 303 nm) was acquired with a scan rate of 0.5 deg per min (from 20 to 90 °C). Faster or slower scan rates did not change the thermal profiles and in all cases forward and backward (from 90 to 20 °C) scans overlapped indicating true equilibrium reactions. The chemical unfolding data was fit to standard equations for two-state reactions [27, 28] to reveal m-values and unfolding-free energies, $\Delta G_U(H_2O)$. Reaction reversibility was tested in all cases. For each protein variant, the far-UV CD (at 220 nm) and tyrosine emission (at 303 nm) data points overlapped in both thermal and chemical reactions. There was no protein-concentration dependence in the transitions (10-50 μM range tested).

Results

Characterization of apo- and holo-forms of CopZ and Atox1

Copper loading of CopZ and target metal-binding domains in Wilson disease protein have been monitored by near-UV CD changes [25, 29]. It has been reported that regardless of Cu(II) or Cu(I) additions, the protein-bound form is always Cu(I) [25, 30-32]. Thus, the copper-binding site must have a considerable preference for Cu(I) over Cu(II), resulting in a high redox potential for the Cu(II)/Cu(I) couple. This is consistent with the principles of hard/soft acid/base theory, which predicts that soft cysteine-thiol ligands have a preference for soft metals such as Cu(I) [33]. In the presence of a reducing agent such as DTT, copper is reduced prior to protein incorporation. In the absence of DTT or other reducing agents, the source of electrons is not known although copper auto-oxidation/reduction has been proposed [25]. We used Ellman's assay to estimate the amount of reduced cysteine thiols in CopZ after sub-stoichiometric additions of Cu(II) in the absence of DTT. Based on our results, it appears that protein-thiol oxidation may not be the major source of electrons for Cu reduction in the absence of exogenous reducing agents (data not shown).

Copper titrations to apo-CopZ monitored by near-UV CD demonstrate the formation of distinct protein-copper complexes: addition of Cu(II) in the absence of reducing agent results in a holo-protein complex proposed to involve two proteins bridged by copper *via* the cysteine residues [25]. In contrast, addition of 1 equivalent of Cu(II) in the presence of DTT creates a monomeric 1:1 holo-form, perhaps involving DTT as an exogenous copper ligand in addition to the two cysteine thiolates (Figure 2A) [19, 34]. We note that the latter species (*i.e.*, the 1:1 complex) may be the most relevant as the cytoplasmic milieu, where these proteins reside, is reducing. *In vivo*, glutathione may acts as a third copper ligand [35] (instead of DTT) or the metal may be two-coordinated using only the protein cysteines [9].

In CopZ, Tyr65 is positioned close to the copper site, *i.e.*, within 7-8 Å [25, 36]. In accord, we found that copper additions to CopZ result in emission quenching until 1:1 stoichiometry is reached (with DTT; Figure 2B). Although copper binding is in essence stoichiometric at these conditions, a protein-copper dissociation constant of about 0.2±0.1 μM (pH 7, 20 °C) could be derived from the fluorescence data. Notably, this value is in good agreement with a previous estimate for CopZ [25].

The copper-binding behavior of apo-Atox1 parallels that of CopZ when monitored by near-UV CD and tyrosine emission changes (data not shown). However, due to the longer distance between the copper site and the tyrosines (see Figure 1), the emission quenching upon copper binding is less for Atox1 (*i.e.*, emission quenched by ~30 % in Atox1 as compared to ~70 % in CopZ). Nonetheless, in the presence of DTT, copper binding levels off at 1:1 ratios when monitored by fluorescence and near-UV CD signals, indicative of a 1:1 Cu(I):Atox1 complex. A previous calorimetric study reported 1:1 Cu(I) binding to Atox1 and a dissociation constant for the complex of about 5 μM (in MES buffer, pH 6.5, 22° C) [24]. In all our experiments with Atox1, therefore, the protein concentration was kept above 20 μM to assure stoichiometric Cu(I) binding. For both Atox1 and CopZ, we verified the presence of stable 1:1 copper-to-protein complexes by dialysis experiments (1 mM DTT, 20 mM Tris, pH 7.5, 20 °C) followed by copper quantification using a biquinoline assay [37].

Chemical unfolding of CopZ and Atox1

Several buffer conditions were evaluated to assure apo- and holo-forms unfolded reversibly and copper ions did not precipitate (final solvent conditions selected for our work include 20 mM Tris, 1 mM DTT, at pH 7.5). Equilibrium unfolding of CopZ and Atox1 was induced by additions of the chemical denaturant, guanidine hydrochloride (GuHCl). Progress of the reactions was monitored by far-UV CD, probing secondary structure, and tyrosine emission, monitoring tertiary structure (Figure 2CD). We found that unfolding of the apo- and monomeric (*i.e.*, 1:1 copper:protein form in the presence of DTT) holo-forms of CopZ and Atox1 are reversible two-state transitions: the CD and fluorescence-detected unfolding data overlap in each case. The holo-forms are more resistant towards chemical perturbation as compared to their corresponding apo-variants (Figure 3AB). Both the GuHCl concentrations at the transition midpoints, and the corresponding unfolding-free energies, are increased in the presence of the metal (Table 1). For

all GuHCl-induced unfolding reactions, the reversibility was tested by denaturant jumps to lower GuHCl concentrations favoring the folded states. For both Atox1 and CopZ, the reactions were over 90 % reversible (data not shown).

Although the unfolding midpoints appear at higher GuHCl concentrations for CopZ than for Atox1, the lower m-value (corresponding to the relative amount of hydrophobic surface-area exposed upon unfolding [27, 28]) results in a lower unfolding-free energy for CopZ as compared to Atox1 (Table 1). This implies that Atox1 has a more well-ordered structure in the native state (regardless of the presence/absence of the metal). This agrees with the NMR data implying more conformational averaging in the apo-form of CopZ than in the apo-form of Atox1 [19, 31, 36].

Thermal unfolding of CopZ and Atox1

Equilibrium unfolding of CopZ and Atox1 was also induced by heating; again, progress of the reactions was monitored by far-UV CD and tyrosine emission (Figure 3CD). Thermal unfolding of the apo- and monomeric holo-forms of CopZ and Atox1 are also reversible two-state transitions in the presence of DTT: the CD and fluorescence-detected unfolding data overlap in each case. Interestingly, CopZ is significantly less stable than Atox1 towards thermal perturbation (T_m of 45 *vs.* 68 °C; Table 1) and the transitions are broader. This agrees with the observation that chemically-induced unfolding of CopZ is less cooperative than of Atox1. Whereas CopZ is stabilized by ~10 °C by the copper, the thermal curves are only shifted by a few degrees when comparing apo- and holo-Atox1 (Figure 3CD). Thermal reversibility was investigated by reverse scans from high to low temperatures monitoring the return of the far-UV CD signal. At the solvent conditions used here, all thermal unfolding processes were over 90 % reversible. We note that heating without DTT resulted in irreversible protein-unfolding profiles, most likely due to copper-mediated thiol oxidation at high temperatures. Thus, it was not possible to assess the thermal stability of the dimeric holo-CopZ complex formed in the absence of added reducing agent.

Discussion

This is the first thermodynamic analysis of copper chaperone unfolding and stability *in vitro*. Depending on copper availability, these proteins cycle between apo- and holo-forms *in vivo.* Therefore, folding and stability properties of both forms are important to understand how these parameters are related to the mechanism of copper transport as well as to diseases caused by mutations in the involved proteins [6, 14, 38-40]. A recent comparative structural-genomic analysis of metallochaperones and metal-transporting ATPases noted several distinctions in terms of residue substitutions and electrostatic/hydrophobic patterns among these otherwise homologous proteins that was proposed to specify partner recognition [15]. Our biophysical observations on Atox1 and CopZ have several implications for the function of copper-transport proteins, as described below.

First, despite the same overall structure, the apo-form of CopZ has a 23-degree lower thermal stability as compared to the apo-form of Atox1. Variations in surface-charges may explain this difference between the proteins on a molecular level [15]. Atox1 and CopZ share only 15 % sequence identity; whereas CopZ is acidic, Atox1 has an isoelectric point of about 7 [15]. Moreover, CopZ has a large patch of negative charges on one side that are proposed to be involved in target recognition (*i.e.*, the metal-binding domains of the *B. subtilis* ATPase CopA). In contrast, the electrostatic surface pattern on Atox1 is more varied, involving many small positive and negative areas. The distribution of charges may allow for the formation of stabilizing salt-bridges on the surface of Atox1 but not in the case of CopZ. As charge-charge interactions become stronger, relative to hydrophobic interactions, at high temperatures [41], their effect on protein stability will be more pronounced in the thermal unfolding experiments; in accord, this is the trend that was observed (Table 1). From a functional perspective, the presence of competing copper chaperones in mammalian cells [1] may require a more stable apo-form in eukaryotes as compared to in prokaryotes.

Second, although the copper-site is located in a loop at the protein surface, copper binding favorably affects both thermal (ΔT_m of 3-10 degrees; pH 7.5) and chemical ($\Delta G(H_2O)$ increases by ~15 %; pH 7.5, 20°C) stability of the two proteins. This phenomenon suggests that copper-binding induces rearrangements throughout the protein structure that improves overall stability. This is in accord with the reported solution structures for these proteins. By NMR, major changes in hydrophobic interactions between secondary structure elements as a function of copper were demonstrated in both CopZ [36] and yeast Atx1 [21]. That the stabilizing effect of metallation is not as dramatic in Atox1 as in CopZ is also reasonable. NMR experiments have revealed that, in contrast to the other chaperones, there are only minor alterations in the Atox1 structure upon copper-binding [31]. The effects of copper-binding on protein stability have been found to vary dramatically. For example, the copper in *Pseudomonas aeruginosa* azurin stabilizes the protein towards chemical perturbations by ~30 % in its reduced form and by 100 % in the oxidized form [42-44]. The copper cofactors also contribute largely to the stability of ascorbate oxidase and Cu,Zn-superoxide dismutase [45, 46] whereas, in the multi-domain enzyme ceruloplasmin, the coppers do not contribute at all to the overall stability [47]. On the contrary, copper was found to promote transitions in the prion protein towards less stable conformations [48] and to coordinate to non-native states of beta-2-microglobulin that resulted in native-state destabilization [49].

Third, since copper has a stabilizing effect on both Atox1 and CopZ, albeit the magnitudes differ, we propose that this is a general trend that applies to copper chaperones and target metal-binding domains in most organisms. In support of this idea, unfolding data on the first metal-binding domain of the human Menkes disease protein (with the same fold as CopZ and Atox1) demonstrates that Cu(I) has a stabilizing effect (T_m differs by ~10 °C for apo- and holo-forms; unpublished data). We propose that differential stability of apo- and holo-forms is linked to conformational/dynamic differences in the copper-binding loop and nearby peptide regions that, in turn, provide a mechanism for *in vivo* target recognition. Copper transfer from the holo-form of the chaperone to the apo-form of the target domain may involve partial chaperone unfolding that is coupled to metal release. Based on our CopZ and Atox1 data, it appears that differential stability (and thus flexibility) of the apo- versus holo-forms are fine-tuned by sequence variations to meet the specific need of each organism.

Interestingly, copper-stimulated proteolysis seems to play an important role in the regulation of copper homeostasis in *Enterococcus hirae* [50-52]. *E. hirae* CopZ was found to be more susceptible to degradation in the copper-bound form than in the apo-form [53]. Copper-induced degradation of the copper transporter Ctr1p of *Saccharomyces cerevisiae* and the yeast transcription factor Mac1, involved in high affinity copper uptake, have also been reported [54, 55]. It is not clear how preferred degradation of the holo-form of *E. hirae* CopZ occurs and what is the identity of the involved protease [53]. Our biophysical results on *B. subtilis* CopZ imply that a protease-recognition mechanism involving protein unfolding is not likely, as we found the holo-form to be more stable than the apo-form. This is reasonable as many proteins can exist in unfolded forms *in vivo* without degradation. Notably, the apo-form of metallothionein was recently found to be present in high levels in human tissues [56-58]. Moreover, although the apo-form of metallothionein is unfolded [59], the folded metal-form (like holo-CopZ in *E. hirae*) appeared less resistant to proteolysis than the apo-form [57].

Finally, from a technical standpoint, our discovery of metal-dependent fluorescence of these copper-chaperones will allow for real time spectroscopic investigations of metal transfer between CopZ/Atox1 and selected target metal-binding domains (work in progress). Notably, the target metal-binding domains of bacterial CopA as well as the human Wilson and Menkes disease proteins do not have tyrosines at the same positions, *i.e.*, near the metal sites, as in CopZ and Atox1 [15].

Acknowledgements

We thank Dr. N. Le Brun and Dr. A. Rosenzweig for the CopZ and Atox1 plasmid constructs, respectively. Support for this project was provided by the Robert A. Welch Foundation (C-1588) and the USAMRAA (Concept award; W81XWH-06-1-0572).

Table 1.
Thermal and chemical (20°C) unfolding data for CopZ and Atox1 with and without copper (Figure 3; 1 mM DTT, 20 mM Tris, pH 7.5). $\Delta G_U(H_2O)$ and m-values were obtained from two-state fits to the data [27, 28]; all reactions were reversible. Individual fits to the CD (at 220 nm) and emission (at 303 nm; excitation at 280 nm) data as a function of GuHCl gave identical parameters for each variant (fits to CD data reported here). * Unit is: kJ/(mol·M).

Protein	**T_m**	**$[GuHCl]_{1/2}$**	**$\Delta G_U(H_2O)$**	**m***
Apo CopZ	45±1°C	2.3±0.1M	13.4±0.5kJ/mol	5.7
Holo CopZ	55±1°C	3.0±0.1M	15.5±0.5kJ/mol	5.1
Apo Atox1	68±1°C	1.8±0.1M	14.5±0.6kJ/mol	7.9
Holo Atox1	71±1°C	2.3±0.1M	16.7±0.7kJ/mol	7.2

Figure legends
Figure 1.
Structures of CopZ (1KOV; left) and Atox1 (1TL4; right). Copper, blue; metal-binding cysteines, red; tyrosines (Tyr65 in CopZ; Tyr64 and Tyr31 in Atox1), orange.
Figure 2.
A. Near-UV CD of apo- (red) and holo-forms of CopZ: 1:2 (light blue; no DTT) and 1:1 (dark blue, 1 mM DTT) copper-to-protein complexes (pH 7.5, 20 °C). **B.** Copper additions to apo-CopZ monitored by fluorescence changes at 303 nm (pH 7.5, 20 °C). **C.** Far-UV CD spectra of folded (red; buffer, pH 7.5, 20 °C) and unfolded (gold; 5 M GuHCl, pH 7.5, 20 °C) forms of apo-CopZ. **Inset C:** Fluorescence spectra of folded (red; buffer, pH 7.5, 20 °C) and unfolded (gold; 5 M GuHCl, pH 7.5, 20 °C) forms of apo-CopZ. **D.** Far-UV CD spectra of folded (blue; buffer, pH 7.5, 20 °C) and unfolded (gold; 5 M GuHCl, pH 7.5, 20 °C) forms of holo-CopZ. **Inset D:** Fluorescence spectra of folded (blue; buffer, pH 7.5, 20 °C) and unfolded (gold; 5 M GuHCl, pH 7.5, 20 °C) forms of holo-CopZ. Similar CD and emission spectra as in C and D were collected for folded and unfolded forms of apo- and holo-Atox1. Whereas the fluorescence decreases for the apo-forms upon unfolding, due to tyrosine exposure to solvent, the emission increases upon unfolding of the holo-forms as the fluorescence is quenched by the copper in the folded state.
Figure 3.
AB. GuHCl-induced unfolding of apo- (circles) and holo- (squares) forms of CopZ (**A**) and Atox1 (**B**) monitored by far-UV CD. Solid curves are two-state fits to the data. **CD.** Thermally-induced unfolding of apo- (red) and holo- (blue) forms of CopZ (**C**) and Atox1 (**D**) monitored by far-UV CD. In all cases, the holo-form corresponds to 1:1 Cu-to-protein ratio in the presence of 1 mM DTT.

References

[1] T.V. O'Halloran and V.C. Culotta, Metallochaperones, an intracellular shuttle service for metal ions, J Biol Chem 275 (2000) 25057-60.

[2] D.L. Huffman and T.V. O'Halloran, Function, structure, and mechanism of intracellular copper trafficking proteins, Annu Rev Biochem 70 (2001) 677-701.

[3] S. Puig, E.M. Rees and D.J. Thiele, The ABCDs of periplasmic copper trafficking, Structure 10 (2002) 1292-5.

[4] S. Puig and D.J. Thiele, Molecular mechanisms of copper uptake and distribution, Curr Opin Chem Biol 6 (2002) 171-80.

[5] E.D. Harris, Basic and clinical aspects of copper, Crit Rev Clin Lab Sci 40 (2003) 547-86.

[6] P.P. Kulkarni, Y.M. She, S.D. Smith, E.A. Roberts and B. Sarkar, Proteomics of metal transport and metal-associated diseases, Chemistry 12 (2006) 2410-22.

[7] A.L. Lamb, A.K. Wernimont, R.A. Pufahl, V.C. Culotta, T.V. O'Halloran and A.C. Rosenzweig, Crystal structure of the copper chaperone for superoxide dismutase, Nat Struct Biol 6 (1999) 724-9.

[8] A.L. Lamb, A.S. Torres, T.V. O'Halloran and A.C. Rosenzweig, Heterodimeric structure of superoxide dismutase in complex with its metallochaperone, Nat Struct Biol 8 (2001) 751-5.

[9] M.D. Harrison, C.E. Jones, M. Solioz and C.T. Dameron, Intracellular copper routing: the role of copper chaperones, Trends Biochem Sci 25 (2000) 29-32.

[10] I. Hamza, M. Schaefer, L.W. Klomp and J.D. Gitlin, Interaction of the copper chaperone HAH1 with the Wilson disease protein is essential for copper homeostasis, Proc Natl Acad Sci U S A 96 (1999) 13363-8.

[11] I.H. Hung, R.L. Casareno, G. Labesse, F.S. Mathews and J.D. Gitlin, HAH1 is a copper-binding protein with distinct amino acid residues mediating copper homeostasis and antioxidant defense, J Biol Chem 273 (1998) 1749-54.

[12] L.W. Klomp, S.J. Lin, D.S. Yuan, R.D. Klausner, V.C. Culotta and J.D. Gitlin, Identification and functional expression of HAH1, a novel human gene involved in copper homeostasis, J Biol Chem 272 (1997) 9221-6.

[13] I.H. Hung, M. Suzuki, Y. Yamaguchi, D.S. Yuan, R.D. Klausner and J.D. Gitlin, Biochemical characterization of the Wilson disease protein and functional expression in the yeast Saccharomyces cerevisiae, J Biol Chem 272 (1997) 21461-6.

[14] N.E. Hellman, S. Kono, G.M. Mancini, A.J. Hoogeboom, G.J. De Jong and J.D. Gitlin, Mechanisms of copper incorporation into human ceruloplasmin, J Biol Chem 277 (2002) 46632-8.

[15] F. Arnesano, L. Banci, I. Bertini, S. Ciofi-Baffoni, E. Molteni, D.L. Huffman and T.V. O'Halloran, Metallochaperones and metal-transporting ATPases: a comparative analysis of sequences and structures, Genome Res 12 (2002) 255-71.

[16] A.C. Rosenzweig, D.L. Huffman, M.Y. Hou, A.K. Wernimont, R.A. Pufahl and T.V. O'Halloran, Crystal structure of the Atx1 metallochaperone protein at 1.02 A resolution, Structure Fold Des 7 (1999) 605-17.

[17] T.M. DeSilva, G. Veglia and S.J. Opella, Solution structures of the reduced and Cu(I) bound forms of the first metal binding sequence of ATP7A associated with Menkes disease, Proteins 61 (2005) 1038-49.

[18] L. Banci, I. Bertini, S. Ciofi-Baffoni, D.L. Huffman and T.V. O'Halloran, Solution structure of the yeast copper transporter domain Ccc2a in the apo and Cu(I)-loaded states, J Biol Chem 276 (2001) 8415-26.

[19] L. Banci, I. Bertini, R. Del Conte, J. Markey and F.J. Ruiz-Duenas, Copper trafficking: the solution structure of Bacillus subtilis CopZ, Biochemistry 40 (2001) 15660-8.

[20] R.A. Pufahl, C.P. Singer, K.L. Peariso, S.J. Lin, P.J. Schmidt, C.J. Fahrni, V.C. Culotta, J.E. Penner-Hahn and T.V. O'Halloran, Metal ion chaperone function of the soluble Cu(I) receptor Atx1, Science 278 (1997) 853-6.
[21] F. Arnesano, L. Banci, I. Bertini, D.L. Huffman and T.V. O'Halloran, Solution structure of the Cu(I) and apo forms of the yeast metallochaperone, Atx1, Biochemistry 40 (2001) 1528-39.
[22] L. Banci, I. Bertini, S. Ciofi-Baffoni, L. Gonnelli and X.C. Su, A core mutation affecting the folding properties of a soluble domain of the ATPase protein CopA from Bacillus subtilis, J Mol Biol 331 (2003) 473-84.
[23] D. Achila, L. Banci, I. Bertini, J. Bunce, S. Ciofi-Baffoni and D.L. Huffman, Structure of human Wilson protein domains 5 and 6 and their interplay with domain 4 and the copper chaperone HAH1 in copper uptake, Proc Natl Acad Sci U S A 103 (2006) 5729-34.
[24] A.K. Wernimont, L.A. Yatsunyk and A.C. Rosenzweig, Binding of copper(I) by the Wilson disease protein and its copper chaperone, J Biol Chem 279 (2004) 12269-76.
[25] M.A. Kihlken, A.P. Leech and N.E. Le Brun, Copper-mediated dimerization of CopZ, a predicted copper chaperone from Bacillus subtilis, Biochem J 368 (2002) 729-39.
[26] M. Ralle, S. Lutsenko and N.J. Blackburn, Copper transfer to the N-terminal domain of the Wilson disease protein (ATP7B): X-ray absorption spectroscopy of reconstituted and chaperone-loaded metal binding domains and their interaction with exogenous ligands, J Inorg Biochem 98 (2004) 765-74.
[27] A. Fersht, Structure and mechanism in protein science, W.H. Freeman and Company, New York, 1999.
[28] C.N. Pace and K.L. Shaw, Linear extrapolation method of analyzing solvent denaturation curves, Proteins Suppl 4 (2000) 1-7.
[29] M. DiDonato, H.F. Hsu, S. Narindrasorasak, L. Que, Jr. and B. Sarkar, Copper-induced conformational changes in the N-terminal domain of the Wilson disease copper-transporting ATPase, Biochemistry 39 (2000) 1890-6.
[30] A. Urvoas, B. Amekraz, C. Moulin, L. Le Clainche, R. Stocklin and M. Moutiez, Analysis of the metal-binding selectivity of the metallochaperone CopZ from Enterococcus hirae by electrospray ionization mass spectrometry, Rapid Commun Mass Spectrom 17 (2003) 1889-96.
[31] I. Anastassopoulou, L. Banci, I. Bertini, F. Cantini, E. Katsari and A. Rosato, Solution structure of the apo and copper(I)-loaded human metallochaperone HAH1, Biochemistry 43 (2004) 13046-53.
[32] V. Tanchou, F. Gas, A. Urvoas, F. Cougouluegne, S. Ruat, O. Averseng and E. Quemeneur, Copper-mediated homo-dimerisation for the HAH1 metallochaperone, Biochem Biophys Res Commun 325 (2004) 388-94.
[33] I. Bertini, H.B. Gary, S.J. Lippard and J.S. Valentine, Bioinorganic Chemistry, University Science Books, Mill Valley, CA, 1994.
[34] M. Ralle, S. Lutsenko and N.J. Blackburn, X-ray absorption spectroscopy of the copper chaperone HAH1 reveals a linear two-coordinate Cu(I) center capable of adduct formation with exogenous thiols and phosphines, J Biol Chem 278 (2003) 23163-70.
[35] A. Urvoas, M. Moutiez, C. Estienne, J. Couprie, E. Mintz and L. Le Clainche, Metal-binding stoichiometry and selectivity of the copper chaperone CopZ from Enterococcus hirae, Eur J Biochem 271 (2004) 993-1003.
[36] L. Banci, I. Bertini and R. Del Conte, Solution structure of apo CopZ from Bacillus subtilis: further analysis of the changes associated with the presence of copper, Biochemistry 42 (2003) 13422-8.
[37] G. Felsenfeld, The determination of cuprous ion in copper proteins, Arch Biochem Biophys 87 (1960) 247-51.

[38] H. Miyajima, Y. Takahashi, T. Kamata, H. Shimizu, N. Sakai and J.D. Gitlin, Use of desferrioxamine in the treatment of aceruloplasminemia, Ann Neurol 41 (1997) 404-7.
[39] J.D. Gitlin, Wilson disease, Gastroenterology 125 (2003) 1868-77.
[40] T.Y. Tao and J.D. Gitlin, Hepatic copper metabolism: insights from genetic disease, Hepatology 37 (2003) 1241-7.
[41] D. Xu, S. Lin and R. Nussinov, Protein binding versus protein folding: The role of hydrophilic bridges in protein associations, JOURNAL OF MOLECULAR BIOLOGY 265 (1997) 68-84.
[42] J. Leckner, P. Wittung, N. Bonander, G. Karlsson and B. Malmstrom, The effect of redox state on the folding free energy of azurin, J. Biol. Inorg. Chem. 2 (1997) 368-371.
[43] P. Wittung-Stafshede, Role of cofactors in folding of the blue-copper protein azurin, Inorg Chem 43 (2004) 7926-33.
[44] P. Wittung-Stafshede, Role of cofactors in protein folding, Acc Chem Res 35 (2002) 201-8.
[45] J.A. Rodriguez, J.S. Valentine, D.K. Eggers, J.A. Roe, A. Tiwari, R.H. Brown, Jr. and L.J. Hayward, Familial amyotrophic lateral sclerosis-associated mutations decrease the thermal stability of distinctly metallated species of human copper/zinc superoxide dismutase, J Biol Chem 277 (2002) 15932-7.
[46] I. Savini, S. D'Alessio, A. Giartosio, L. Morpurgo and L. Avigliano, The role of copper in the stability of ascorbate oxidase towards denaturing agents, Eur J Biochem 190 (1990) 491-5.
[47] E. Sedlak, Wittung-Stafshede, P, Role of copper ions in chemical unfolding of human ceruloplasmin, Biochemistry in press (2007).
[48] J. Stockel, J. Safar, A.C. Wallace, F.E. Cohen and S.B. Prusiner, Prion protein selectively binds copper(II) ions, Biochemistry 37 (1998) 7185-93.
[49] C.M. Eakin, J.D. Knight, C.J. Morgan, M.A. Gelfand and A.D. Miranker, Formation of a copper specific binding site in non-native states of beta-2-microglobulin, Biochemistry 41 (2002) 10646-56.
[50] Z.H. Lu, C.T. Dameron and M. Solioz, The Enterococcus hirae paradigm of copper homeostasis: copper chaperone turnover, interactions, and transactions, Biometals 16 (2003) 137-43.
[51] M. Solioz, Role of proteolysis in copper homoeostasis, Biochem Soc Trans 30 (2002) 688-91.
[52] M. Solioz and J.V. Stoyanov, Copper homeostasis in Enterococcus hirae, FEMS Microbiol Rev 27 (2003) 183-95.
[53] Z.H. Lu and M. Solioz, Copper-induced proteolysis of the CopZ copper chaperone of Enterococcus hirae, J Biol Chem 276 (2001) 47822-7.
[54] C.E. Ooi, E. Rabinovich, A. Dancis, J.S. Bonifacino and R.D. Klausner, Copper-dependent degradation of the Saccharomyces cerevisiae plasma membrane copper transporter Ctr1p in the apparent absence of endocytosis, Embo J 15 (1996) 3515-23.
[55] Z. Zhu, S. Labbe, M.M. Pena and D.J. Thiele, Copper differentially regulates the activity and degradation of yeast Mac1 transcription factor, J Biol Chem 273 (1998) 1277-80.
[56] Y. Yang, W. Maret and B.L. Vallee, Differential fluorescence labeling of cysteinyl clusters uncovers high tissue levels of thionein, Proc Natl Acad Sci U S A 98 (2001) 5556-9.
[57] D.H. Petering, J. Zhu, S. Krezoski, J. Meeusen, C. Kiekenbush, S. Krull, T. Specher and M. Dughish, Apo-metallothionein emerging as a major player in the cellular activities of metallothionein, Exp Biol Med (Maywood) 231 (2006) 1528-34.
[58] A. Krezel and W. Maret, Different redox states of metallothionein/thionein in biological tissue, Biochem J 402 (2007) 551-8.

[59] J. Ejnik, J. Robinson, J. Zhu, H. Forsterling, C.F. Shaw and D.H. Petering, Folding pathway of apo-metallothionein induced by Zn2+, Cd2+ and Co2+, J Inorg Biochem 88 (2002) 144-52.

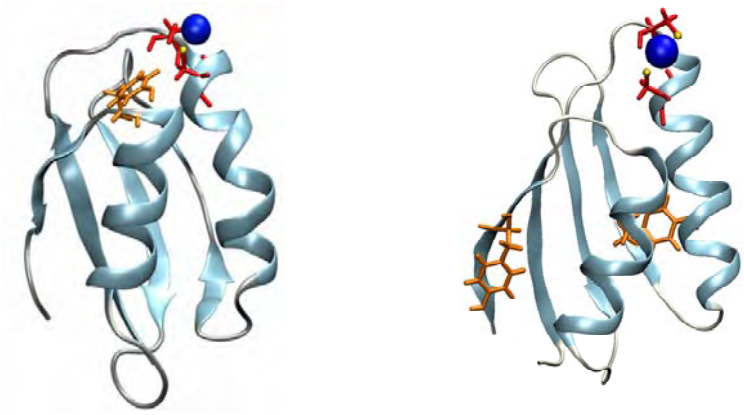

Figure 1

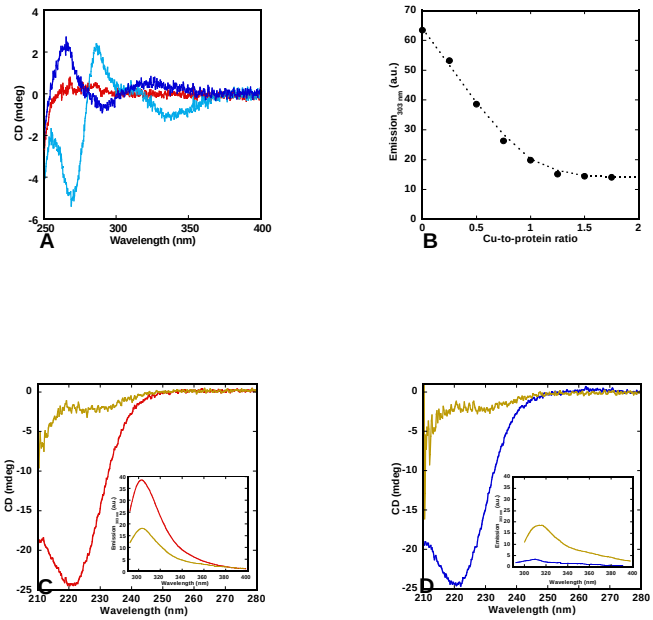

Figure 2

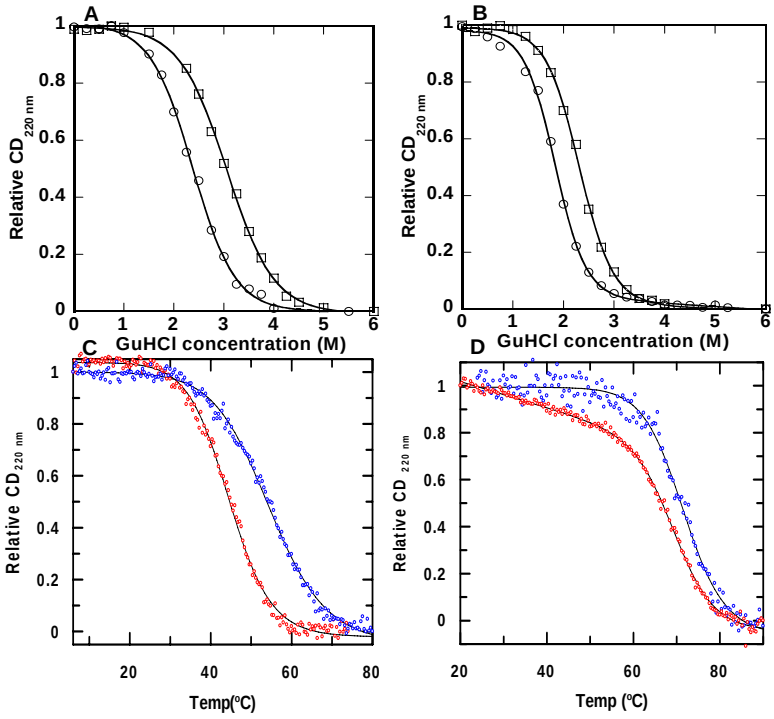

Figure 3